



# SARS-CoV-2 spike conformation determines plasma neutralizing activity elicited by a wide panel of human vaccines

## Journal Article

### Author(s):

Bowen, John E.; Park, Young-Jun; Stewart, Cameron; Brown, Jack T.; Sharkey, William K.; Walls, Alexandra C.; Joshi, Anshu; Sprouse, Kaitlin R.; McCallum, Matthew; Tortorici, M. Alejandra; Franko, Nicholas M.; Logue, Jennifer K.; Mazzitelli, Ignacio G.; Nguyen, Annalee W.; Silva, Rui P.; Huang, Yimin; [Low, Jun Siong](#) ; Jerak, Josipa; Tiles, Sasha W.; Ahmed, Kumail; [Sallusto, Federica](#) ; et al.

### Publication date:

2022-12

### Permanent link:

<https://doi.org/10.3929/ethz-b-000596105>

### Rights / license:

[Creative Commons Attribution 4.0 International](#)

### Originally published in:

Science Immunology 7(78), <https://doi.org/10.1126/sciimmunol.adf1421>

## CORONAVIRUS

# SARS-CoV-2 spike conformation determines plasma neutralizing activity elicited by a wide panel of human vaccines

John E. Bowen<sup>1</sup>, Young-Jun Park<sup>1,2</sup>, Cameron Stewart<sup>1</sup>, Jack T. Brown<sup>1</sup>, William K. Sharkey<sup>1</sup>, Alexandra C. Walls<sup>1,2</sup>, Anshu Joshi<sup>1</sup>, Kaitlin R. Sprouse<sup>1</sup>, Matthew McCallum<sup>1</sup>, M. Alejandra Tortorici<sup>1</sup>, Nicholas M. Franko<sup>3</sup>, Jennifer K. Logue<sup>3</sup>, Ignacio G. Mazzitelli<sup>4</sup>, Annalee W. Nguyen<sup>5</sup>, Rui P. Silva<sup>5</sup>, Yimin Huang<sup>5</sup>, Jun Siong Low<sup>6</sup>, Josipa Jerak<sup>6</sup>, Sasha W. Tiles<sup>7</sup>, Kumail Ahmed<sup>8</sup>, Asefa Shariq<sup>8</sup>, Jennifer M. Dan<sup>9,10</sup>, Zeli Zhang<sup>9,10</sup>, Daniela Weiskopf<sup>9,10</sup>, Alessandro Sette<sup>9,10</sup>, Gyorgy Snell<sup>11</sup>, Christine M. Posavad<sup>12</sup>, Najeeha Talat Iqbal<sup>8</sup>, Jorge Geffner<sup>4</sup>, Alessandra Bandera<sup>13</sup>, Andrea Gori<sup>13</sup>, Federica Sallusto<sup>6</sup>, Jennifer A. Maynard<sup>5</sup>, Shane Crotty<sup>9,10</sup>, Wesley C. Van Voorhis<sup>7</sup>, Carlos Simmerling<sup>14,15</sup>, Renata Grifantini<sup>16</sup>, Helen Y. Chu<sup>3</sup>, Davide Corti<sup>17</sup>, David Veesler<sup>1,2\*</sup>

Numerous safe and effective coronavirus disease 2019 vaccines have been developed worldwide that use various delivery technologies and engineering strategies. We show here that vaccines containing prefusion-stabilizing S mutations elicit antibody responses in humans with enhanced recognition of S and the S<sub>1</sub> subunit relative to postfusion S as compared with vaccines lacking these mutations or natural infection. Prefusion S and S<sub>1</sub> antibody binding titers positively and equivalently correlated with neutralizing activity, and depletion of S<sub>1</sub>-directed antibodies completely abrogated plasma neutralizing activity. We show that neutralizing activity is almost entirely directed to the S<sub>1</sub> subunit and that variant cross-neutralization is mediated solely by receptor binding domain-specific antibodies. Our data provide a quantitative framework for guiding future S engineering efforts to develop vaccines with higher resilience to the emergence of variants than current technologies.

## INTRODUCTION

The severe acute respiratory syndrome coronavirus 2 (SARS-CoV-2) spike (S) glycoprotein promotes viral entry into host cells and is the main target of neutralizing antibodies (1, 2). S comprises two functional subunits, designated S<sub>1</sub> and S<sub>2</sub>, that interact noncovalently after furin cleavage during synthesis (1, 3, 4). The receptor binding domain (RBD), which engages the angiotensin-converting enzyme 2 receptor (1, 3, 5–7), and the N-terminal domain (NTD) that recognizes attachment factors (8–10) are components of the S<sub>1</sub>

subunit. The S<sub>2</sub> subunit contains the fusion machinery and undergoes large-scale structural rearrangements from a high-energy spring-loaded prefusion conformation to a postfusion state, driving fusion of the virus and host membranes and initiating infection (11–13). Antibodies that bind to specific sites on the RBD (14–24), the NTD (25–29), or the fusion machinery (30–36) neutralize SARS-CoV-2, and serum neutralizing antibody titers are a correlate of protection (37–43).

As of October 2022, more than 12.8 billion coronavirus disease 2019 (COVID-19) vaccine doses have been administered worldwide. Moderna/National Institute of Allergy and Infectious Diseases (NIAID) mRNA-1273 and Pfizer/BioNTech BNT162b2 were conceived as two-dose vaccines based on an mRNA encoding the full-length prefusion-stabilized “2P” S glycoprotein encapsulated in a lipid nanoparticle (44–46). Novavax NVX-CoV2373 is a prefusion-stabilized 2P S protein subunit vaccine with a mutated furin cleavage site and formulated with a saponin-based matrix M adjuvant (47), whereas AstraZeneca/Oxford AZD1222, Gamaleya Research Institute Sputnik V, and Janssen Ad26.COVS are replication-defective adenoviral-vectored vaccines encoding for the full-length S glycoprotein. Only Ad26.COVS encodes for a prefusion-stabilized S with the 2P mutations and mutated furin cleavage site (48), whereas the other two vaccines lack these modifications. The adenoviral vectors used are chimpanzee AdY25 for AZD1222 (49) and Ad26 (prime)/Ad5 (boost) for Sputnik V (50), both vaccines initially using two doses, and Ad26 for Ad26.COVS, which originated as a single-dose vaccine (48). Sinopharm BBIBP-CorV (51) is an alum-adjuvanted, β-propiolactone-inactivated SARS-CoV-2 viral vaccine that initially used a two-dose regimen.

<sup>1</sup>Department of Biochemistry, University of Washington, Seattle, WA 98195, USA. <sup>2</sup>Howard Hughes Medical Institute, University of Washington, Seattle, WA 98195, USA. <sup>3</sup>Division of Allergy and Infectious Diseases, University of Washington, Seattle, WA 98195, USA. <sup>4</sup>Instituto de Investigaciones Biomédicas en Retrovirus y SIDA (INBIRS), Facultad de Medicina, Buenos Aires C1121ABG, Argentina. <sup>5</sup>McKetta Department of Chemical Engineering, University of Texas at Austin, Austin, TX 78712, USA. <sup>6</sup>Institute for Research in Biomedicine, Università della Svizzera Italiana, 6500 Bellinzona, Switzerland. <sup>7</sup>Center for Emerging and Re-emerging Infectious Diseases, Division of Allergy and Infectious Diseases, Department of Medicine, University of Washington School of Medicine, Seattle, WA 98195, USA. <sup>8</sup>Departments of Paediatrics and Child Health and Biological and Biomedical Sciences, Aga Khan University, Karachi 74800, Pakistan. <sup>9</sup>Center for Infectious Disease and Vaccine Research, La Jolla Institute for Immunology, La Jolla, CA 92037, USA. <sup>10</sup>Division of Infectious Diseases and Global Public Health, Department of Medicine, University of California, San Diego, La Jolla, CA UC92037, USA. <sup>11</sup>Vir Biotechnology, San Francisco, CA 94158, USA. <sup>12</sup>Vaccine and Infectious Disease Division, Fred Hutchinson Cancer Center, Seattle, WA 98109, USA. <sup>13</sup>Infectious Diseases Unit, Fondazione IRCCS Ca' Granda Ospedale Maggiore Policlinico, 20122 Milan, Italy. <sup>14</sup>Department of Chemistry, Stony Brook University, Stony Brook, NY 11794, USA. <sup>15</sup>Laufer Center for Physical and Quantitative Biology, Stony Brook University, Stony Brook, NY 11794, USA. <sup>16</sup>INGM, Istituto Nazionale Genetica Molecolare “Romeo ed Enrica Invernizzi,” 20122 Milan, Italy. <sup>17</sup>Humabs Biomed SA, a subsidiary of Vir Biotechnology, 6500 Bellinzona, Switzerland.

\*Corresponding author. Email: dveesler@uw.edu

Here, we set out to evaluate the influence of the SARS-CoV-2 S glycoprotein conformation on plasma neutralizing activity, which is a correlate of protection against COVID-19. To understand the molecular basis of elicitation of neutralizing antibodies elicited by a wide range of COVID-19 vaccines in humans and how to modulate their magnitude and breadth, we assessed the specificity of S-directed antibody responses, the relationship between antibody binding titers and neutralization potency, and the relative contribution of the RBD and the NTD to vaccine-mismatched cross-neutralizing activity against SARS-CoV-2 variants.

## RESULTS

### Prefusion SARS-CoV-2 S stabilization reduces the fraction of antibodies recognizing an off-target conformational state

To understand the specificity of S-directed antibody responses elicited by vaccination or infection, we evaluated plasma immunoglobulin G (IgG) binding titers against the thoroughly validated prefusion-stabilized SARS-CoV-2 S trimer, the  $S_1$  subunit, the NTD, the RBD, and the  $S_2$  subunit (fusion machinery) in the prefusion [ $S_{2(\text{Pre})}$ ] and postfusion [ $S_{2(\text{Post})}$ ] states (figs. S1 to S3 and table S1). We determined a cryo-electron microscopy (cryoEM) structure of  $S_{2(\text{Pre})}$  that is presented in more detail in figs. S2 and S3 and table S1. Our panel includes samples from individuals who were not previously exposed to SARS-CoV-2 and received two doses of Moderna mRNA-1273, Pfizer/BioNTech BNT162b2, Novavax NVX-CoV2373, Janssen Ad26.COVS.2.S, AstraZeneca AZD1222, Gamaleya Research Institute Sputnik V, or Sinopharm BBIBP-CorV. We benchmarked these samples against COVID-19 human convalescent plasma obtained before January 2021, likely resulting from exposure to a Wuhan-Hu-1-related SARS-CoV-2 strain based on the date of symptom onset (table S2) (52). Individuals who received two doses of mRNA-1273 or BNT162b2 had the highest prefusion S binding titers [geometric mean titers (GMTs) of 8.1 and 7.5, respectively], whereas infected individuals had the lowest and most heterogeneous prefusion S binding titers (GMT of 3.8), as assessed by enzyme-linked immunosorbent assays (ELISAs). Individuals who received two doses of NVX-CoV2373, Ad26.COVS.2.S, AZD1222, Sputnik V, and BBIBP-CorV had intermediate prefusion S binding GMTs (4.8, 5.3, 6.3, 5.0, and 5.2, respectively), although samples of individuals vaccinated with NVX-CoV2373 were collected ~2 to 3 months later than the other cohorts relative to the second vaccine dose (53, 54). A similar trend and cohort grouping from highest (mRNA-1273 and BNT162b2) to intermediate (NVX-CoV2373, Ad26.COVS.2.S, AZD1222, Sputnik V, and BBIBP-CorV) and lowest (infected) binding titers were observed when using the  $S_1$  subunit, the NTD, or the RBD as ELISA antigens (Fig. 1A, figs. S4 and S5, and table S3). Vaccination with two doses of mRNA-1273, BNT162b2, NVX-CoV2373, Ad26.COVS.2.S, AZD1222, and Sputnik V resulted in greater binding titers against  $S_1$  compared with  $S_{2(\text{Pre})}$  and  $S_{2(\text{Post})}$  compared with  $S_{2(\text{Post})}$ , whereas infection or two doses of BBIBP-CorV resulted in greater binding titers against  $S_{2(\text{Post})}$  compared with  $S_{2(\text{Pre})}$  and  $S_{2(\text{Pre})}$  compared with  $S_1$  (Fig. 1A, fig. S5, and table S4).

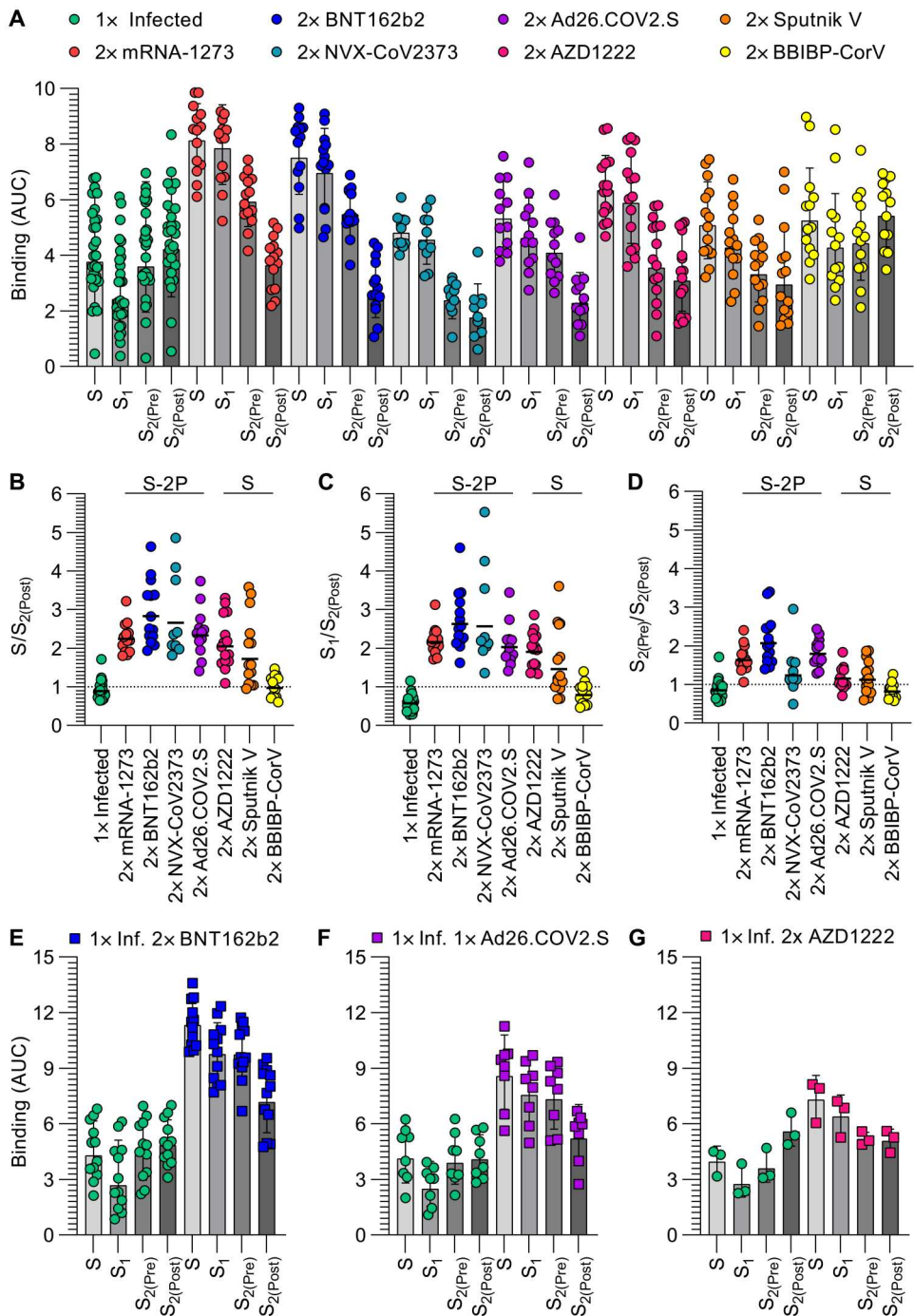
To assess the impact of prefusion S stabilization on vaccine-elicited antibody responses, we compared prefusion S-,  $S_1$ -, and  $S_{2(\text{Pre})}$ -directed antibody titers with postfusion  $S_2$ -directed antibodies across all seven vaccines and infection. Vaccination with two

doses of mRNA-1273, BNT162b2, NVX-CoV2373, or Ad26.COVS.2.S elicited polyclonal plasma antibodies with higher  $S/S_{2(\text{Post})}$  binding ratios (2.2, 2.8, 2.7, and 2.3, respectively) than two doses of AZD1222 and Sputnik V vaccines (2.1 and 1.7, respectively). Infection or two-dose BBIBP-CorV vaccination elicited the lowest  $S/S_{2(\text{Post})}$  ratios (0.9 and 1.0, respectively; Fig. 1B and table S5). This indicates preferential targeting of prefusion S by antibodies elicited by most vaccines and particularly those that contain the 2P prefusion-stabilizing S mutations. Infection resulted in a  $S_1/S_{2(\text{Post})}$  binding ratio of 0.6, whereas a two-dose vaccination with mRNA-1273, BNT162b2, NVX-CoV2373, Ad26.COVS.2.S, AZD1222, Sputnik V, or BBIBP-CorV resulted in  $S_1/S_{2(\text{Post})}$  binding ratios of 2.2, 2.6, 2.6, 2.0, 1.9, 1.5, and 0.8, respectively, thereby following the same trend as  $S/S_{2(\text{Post})}$  binding ratios (Fig. 1C and table S5). Vaccines containing prefusion-stabilizing mutations therefore elicited a higher proportion of S- and  $S_1$ - relative to  $S_{2(\text{Post})}$ -directed polyclonal plasma antibodies compared with vaccines lacking such mutations or infection. Infection resulted in a  $S_{2(\text{Pre})}/S_{2(\text{Post})}$  binding ratio of 0.9, whereas a two-dose vaccination with mRNA-1273, BNT162b2, NVX-CoV2373, Ad26.COVS.2.S, AZD1222, Sputnik V, and BBIBP-CorV elicited  $S_{2(\text{Pre})}/S_{2(\text{Post})}$  binding ratios of 1.6, 2.1, 1.2, 1.8, 1.2, 1.1, and 0.8, respectively (Fig. 1D and table S5). Prefusion-stabilized vaccines therefore elicited comparable or greater prefusion  $S_2$ - over postfusion  $S_2$ -directed antibody responses relative to other vaccines, with the exception of NVX-CoV2373, which was characterized by low  $S_{2(\text{Pre})}$  over  $S_{2(\text{Post})}$  antibody titers, possibly due to the vaccine formulation or later timing of blood draw after the second dose. Collectively, these data point to reduced elicitation of  $S_1$ -directed relative to postfusion  $S_2$ -directed antibodies in infected individuals or two-dose BBIBP-CorV vaccinees. This is likely due to  $S_1$  shedding and  $S_2$  refolding to the postfusion conformation at the surface of authentic virions or infected cells (55–57) or as a result of the  $\beta$ -propiolactone inactivation procedure used by Sinopharm (58).

Previous studies demonstrated that COVID-19 vaccination of individuals previously infected with SARS-CoV-2 elicits high antibody binding and neutralizing titers (59–62). We therefore set out to assess and compare how antibody binding responses are affected upon vaccination of previously infected individuals with two doses of BNT162b2, one dose of Ad26.COVS.2.S, or two doses of AZD1222, corresponding to primary vaccine series dosing schemes. Although vaccination markedly enhanced the magnitude of antibody binding responses against all antigens tested, different vaccines led to distinct magnitudes of boosting. Postvaccination to prevaccination prefusion S binding titers increased 2.6 times after two doses of BNT162b2, 2.1 times after a single dose of Ad26.COVS.2.S, and 1.8 times after two doses of AZD1222 (Fig. 1, E to G; fig. S6; and tables S6 and S7). Whereas we observed  $S/S_{2(\text{Post})}$  binding ratios between 0.7 and 1.0 before vaccination, they rose to 1.6 for BNT162b2 and Ad26.COVS.2.S and to 1.4 for AZD1222 after vaccination (Fig. 1, E to G; fig. S6; and tables S6 and S7). Because of the metastable nature of the S trimer, which is prone to shedding the  $S_1$  subunit and refolding to form postfusion trimers (11, 44, 55, 57, 63), the absence of prefusion-stabilizing S mutations in the AZD1222 vaccine might explain the slightly lower  $S/S_{2(\text{Post})}$  binding ratios relative to BNT162b2 and Ad26.COVS.2.S. These data show that immunization with any of these three vaccines after infection skewed antibody responses preferentially toward prefusion S relative to postfusion  $S_2$ , unlike in infection only.

**Fig. 1. Prefusion SARS-CoV-2 S stabilization reduces the fraction of antibodies recognizing off-target conformational states. (A)** IgG binding titers elicited by SARS-CoV-2 infection or vaccination against prefusion S (S), the S<sub>1</sub> subunit, and the S<sub>2</sub> subunit in the prefusion [S<sub>2(Pre)</sub>] and postfusion [S<sub>2(Post)</sub>] conformations, as measured by ELISA. Statistical analyses are shown in tables S3 and S4. (B to D) Ratios of plasma IgG binding titers against prefusion S (B), the S<sub>1</sub> subunit (C), and the S<sub>2</sub> subunit in the prefusion conformation [S<sub>2(Pre)</sub>] (D) over the plasma IgG binding titers against the S<sub>2</sub> subunit in the postfusion conformation [S<sub>2(Post)</sub>]. Cohorts labeled “S-2P” received vaccines encoding for or containing 2P prefusion-stabilizing S mutations, whereas cohorts labeled “S” received vaccines lacking those mutations. Statistical analysis is shown in table S5. (E to G) IgG binding titers before and after vaccination with two doses of BNT162b2 (E), one dose of Ad26.COVS.2 (F), or two doses of AZD1222 (G) in longitudinal cohorts of individuals previously uninfected with SARS-CoV-2. Statistical analyses are shown in tables S6 and S7. 1× Infected samples (n = 28) were obtained 26 to 78 days (mean, 42) after symptom onset, 2× mRNA-1273 samples (n = 14) were obtained 6 to 50 days (mean, 15) after the second dose, 2× BNT162b2 samples (n = 14) were obtained 6 to 33 days (mean, 14) after the second dose, 2× NVX-CoV2373 samples (n = 10) were obtained 17 to 168 days (mean, 93 to 119) after the second dose, 2× Ad26.COVS.2 samples (n = 12) were obtained 12 to 16 days (mean, 14) after the second dose, 2× AZD1222 samples (n = 15) were obtained ~30 days after the second dose, 2× Sputnik V samples (n = 14) were obtained 60 to 90 days after the second dose, BBIBP-CorV samples (n = 13) were obtained 15 to 102 days (mean, 71) after the second dose, 1× infected 2× BNT162b2 samples (n = 12) were obtained 10 to 32 days (mean, 16) after the second dose, 1× infected 1× Ad26.COVS.2 samples (n = 8) were obtained 12 to 112 days (mean, 38) after the first dose, and 1× infected 2× AZD1222 samples (n = 3) were obtained ~30 days after the second dose. Each point represents a single patient plasma sample from one representative of at least two independent experiments consisting of different antigens, shaded bars represent the geometric mean, and error bars represent the geometric SD. AUC was determined after log-transforming the plasma dilution, and these data are shown in figs. S5 and S6. Patient demographics are shown in table S2.

**SARS-CoV-2 neutralization is determined by S<sub>1</sub> subunit-targeting antibodies**  
 To investigate the relationship between antibody binding titers and neutralization potency, we determined the half-maximum inhibitory dilutions of the aforementioned plasma samples using a vesicular stomatitis virus (VSV) pseudotyped with the Wuhan-Hu-1 S glycoprotein harboring the D614G substitution (G614) and VeroE6 cells stably expressing TMPRSS2 (64). As a direct reflection of prefusion



S and S<sub>1</sub> binding titers, mRNA-1273 and BNT162b2 vaccinee plasma exhibited the highest neutralization potencies (GMTs of 1080 and 968, respectively), whereas the neutralizing activity of previously infected individuals was the weakest among all groups (GMT of 60) (Fig. 2A; fig. S7, A to C; and table S8). Infection elicited the most heterogeneous humoral immune responses as defined by the wide spread of prefusion S binding and associated neutralizing antibody titers compared with other groups (Figs. 1A and 2A).

Downloaded from https://www.science.org at Eth Zurich on February 10, 2023

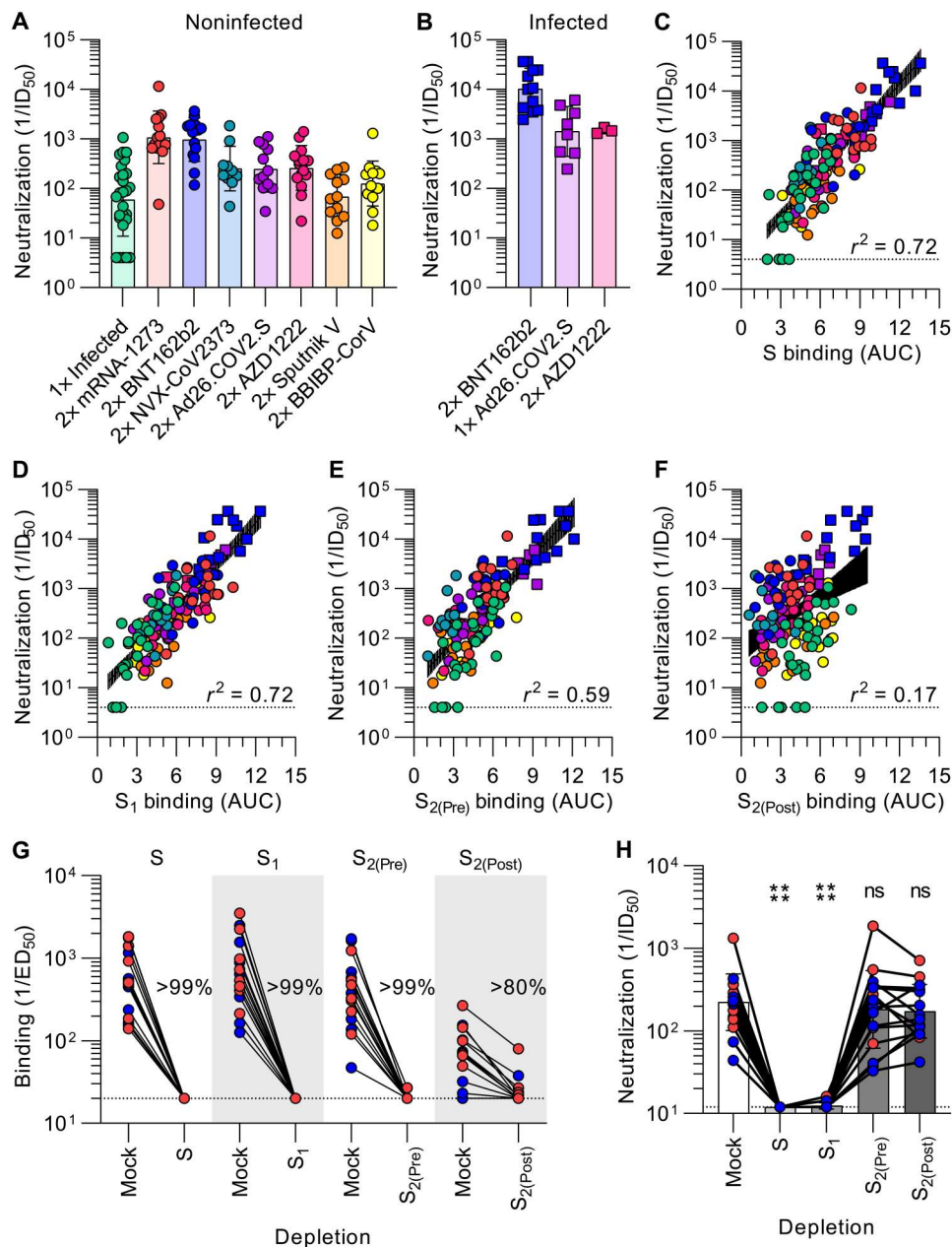


**Fig. 2. SARS-CoV-2 neutralization is determined by S<sub>1</sub> subunit-targeting antibodies.** (A and B) SARS-CoV-2 S pseudotyped VSV neutralization titers elicited by infection or vaccination (A) or vaccination after infection (B). The dotted line is the limit of detection, the colored bars are GMTs, and the black error bars are geometric SDs. Colored points are the neutralizing geometric means of individuals after two to four experimental repeats consisting of different batches of pseudovirus, representative normalized curves are shown in figs. S7 and S8, and statistical analyses are shown in tables S7 and S8. (C to F) Correlation between plasma neutralizing activity and pre-fusion S (C), S<sub>1</sub> (D), pre-fusion S<sub>2</sub> (E), and post-fusion S<sub>2</sub> (F) binding titers shown with a linear regression fit to the log of neutralization titers. The black shaded regions represent 95% confidence intervals.  $P < 0.0001$  for all four panels. (G and H) Binding (G) and neutralization (H) titers resulting from depletion of polyclonal plasma antibodies targeting S, S<sub>1</sub>, pre-fusion S<sub>2</sub>, and post-fusion S<sub>2</sub>. Each point is a patient plasma sample from one representative of two independent experiments consisting of different batches of antigen and pseudovirus, shaded bars represent the geometric mean, and error bars represent the geometric SD. Red points correspond to individuals vaccinated with two doses of mRNA-1273, whereas blue points correspond to individuals vaccinated with two doses of BNT162b2. Statistical significance between groups of data, relative to mock depletion, was determined by ratio paired Wilcoxon rank test and ns (not significant)  $> 0.05$  and  $****P < 0.0001$ . Mock consists of depletion carried out with beads lacking immobilized antigen. Binding data are shown in fig. S10, and dose-response neutralization curves are shown in fig. S11. Patient demographics are shown in table S2. ID<sub>50</sub>, median inhibitory dose.

Individuals vaccinated twice with NVX-CoV2373, Ad26.COV2.S, AZD1222, Sputnik V, or BBIBP-CorV had neutralizing titers of 252, 247, 259, 69, and 126, respectively (Fig. 2A; fig. S7, D to H; and table S8), although we note that NVX-CoV2373 samples were obtained the furthest from peak titers due to the design of the clinical trial from which they were obtained (table S2) (53, 54). Individuals previously exposed to SARS-CoV-2 reached neutralizing GMTs of 10,232 after two doses of BNT162b2 and 1479 after two doses of AZD1222 (Fig. 2B, fig. S8A, and table S9), corresponding to respective increases of 10.5- and 5.7-fold over those who had not been previously exposed to SARS-CoV-2 (59–62). Plasma from individuals previously infected with SARS-CoV-2 reached a neutralizing GMT of 1421 after a single dose of Ad26.COV2.S (Fig. 2B, fig. S8, and table S9), a 5.8-fold enhancement relative to those who received two doses of Ad26.COV2.S. Thus, vaccination of previously infected individuals elicits neutralizing antibody titers greater than administration of two doses of mRNA-1273 or BNT162b2 in naive individuals, in line with previous reports (59–62).

We observed a strong positive correlation between *in vitro* plasma inhibitory activity and the magnitude of antibody responses

against the prefusion-stabilized S trimer for all vaccines evaluated and for infection-elicited polyclonal antibodies (Fig. 2C). Furthermore, we observed a comparable positive correlation between neutralizing activity and S<sub>1</sub> binding antibody responses, suggesting a key role of S<sub>1</sub>-directed antibodies for SARS-CoV-2 neutralization (Fig. 2D). Neutralizing antibody titers were also positively correlated with NTD- and RBD-specific binding titers (fig. S9), in line with these two domains being part of the S<sub>1</sub> subunit and the main targets of neutralizing antibodies upon infection or vaccination (17, 25, 59, 65–67). The rapid accumulation of amino acid residue mutations in the SARS-CoV-2 S<sub>1</sub> subunit throughout the COVID-19 pandemic (68) might therefore reflect, at least in part, the selective pressure exerted by host neutralizing antibodies. Although prefusion S<sub>2</sub> antibody binding titers positively correlated with neutralization potency (Fig. 2E), postfusion S<sub>2</sub> responses did not (Fig. 2F), indicating that antibodies targeting postfusion S are likely weak or not able to block viral entry. These results underscore the benefits of eliciting antibody responses targeting the prefusion S conformation, and particularly the S<sub>1</sub> subunit, to maximize plasma neutralizing activity

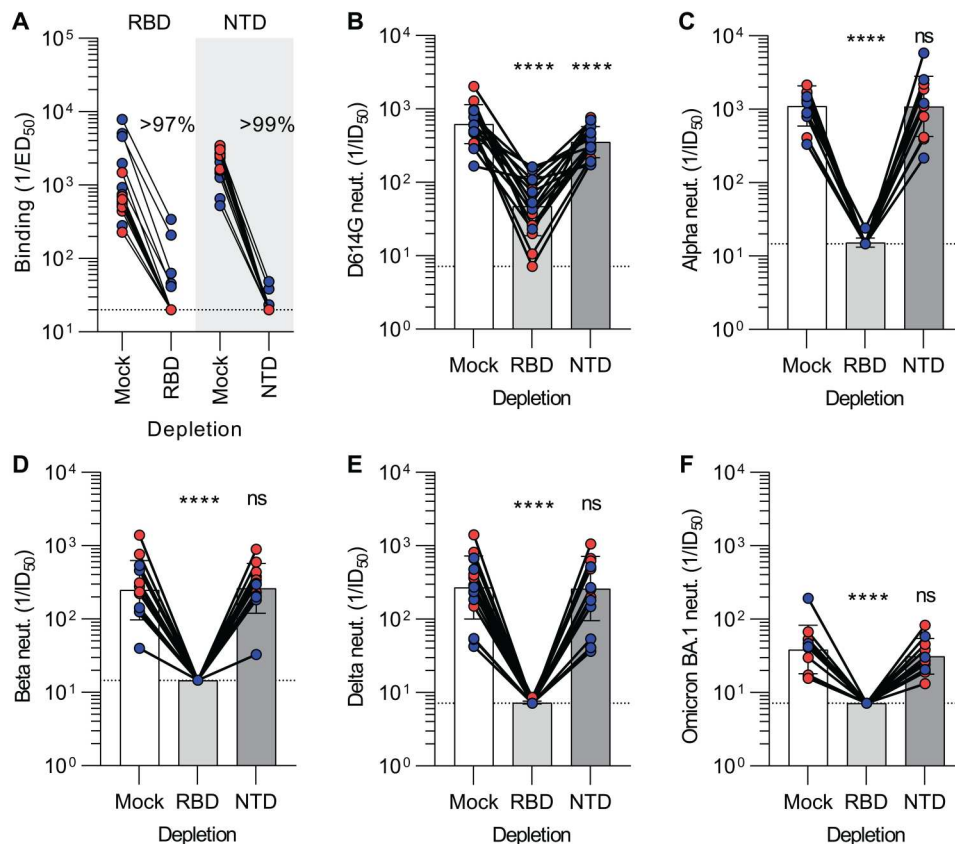


**Fig. 3. Vaccine-elicited broad neutralization of SARS-CoV-2 variants is mediated by RBD-directed antibodies.** (A) Plasma IgG binding titers resulting from mock, Wuhan-Hu-1 RBD (left), and Wuhan-Hu-1 NTD (right) depletion of polyclonal antibodies. ED<sub>50</sub>, 50% effective dose. (B to F) Plasma neutralizing activity against G614 S VSV (B), Alpha S VSV (C), Beta S VSV (D), Delta S VSV (E), and Omicron BA.1 S VSV (F) after mock, Wuhan-Hu-1 RBD, or Wuhan-Hu-1 NTD depletion of polyclonal antibodies. We note that mock-depleted BA.1 S VSV neutralization is dampened relative to G614 S VSV, in agreement with previous findings (53, 83, 84). Each point corresponds to a single patient plasma sample from one representative of two independent experiments consisting of different batches of antigen and pseudovirus, shaded bars represent the geometric mean, and error bars represent the geometric SD. Red points correspond to individuals vaccinated with two doses of mRNA-1273, whereas blue points correspond to individuals vaccinated with two doses of BNT162b2. Mock consists of depletion carried out with beads lacking immobilized antigen. Statistical significance between groups of data, relative to mock depletion, was determined by ratio paired Wilcoxon rank test and ns > 0.05 and \*\*\*\**P* < 0.0001. Fit binding curves are shown in fig. S12, and dose-response neutralization curves are shown in fig. S13. Patient demographics are shown in table S2.

and the higher quality of humoral immune responses elicited by vaccination with most platforms compared with natural infection.

To obtain a quantitative understanding of the relationship between S conformation and plasma neutralizing activity, we depleted polyclonal antibodies using prefusion S, the S<sub>1</sub> subunit, prefusion S<sub>2</sub>, or postfusion S<sub>2</sub> from the plasma of vaccinees who received two doses of mRNA-1273 or of BNT162b2. Binding titers against the respective antigens were reduced by >99% for S, S<sub>1</sub>, and S<sub>2(Pre)</sub> and >80% for S<sub>2(Post)</sub> as determined by ELISA, confirming effective antigen-specific antibody removal (Fig. 2G and fig. S10). Depletion of prefusion S- or S<sub>1</sub> subunit-targeting antibodies resulted in a near-complete loss of neutralizing activity, whereas depletion using prefusion or postfusion S<sub>2</sub> had no detectable impact (Fig. 2H and fig. S11). These results clearly demonstrate that virtually all plasma neutralizing activity targets prefusion S, which is reminiscent of findings made for the respiratory syncytial virus fusion (F) glycoprotein (69, 70). The coronavirus S glycoprotein, however, mediates both receptor binding and membrane fusion, whereas respiratory syncytial virus F solely promotes membrane fusion. Furthermore, our data show that antibodies targeting the S<sub>1</sub> subunit, and not the S<sub>2</sub> subunit, account for vaccine-elicited plasma neutralizing activity. It is therefore S<sub>1</sub> subunit shedding rather than S<sub>2</sub> conformational changes associated with the prefusion to postfusion transition that leads to a marked loss of potency because most neutralizing antibodies target the RBD (17, 65, 71) and the NTD (25, 26, 28).

### SARS-CoV-2 variant cross-neutralization is determined by RBD-specific antibodies

To evaluate the relative contribution of the RBD and the NTD to cross-neutralizing activity against SARS-CoV-2 variants, we depleted mRNA vaccinee plasma samples of antibodies recognizing each of these two antigens (Fig. 3A and fig. S12). Plasma neutralizing activity was subsequently determined against VSV pseudotyped with the G614 S glycoprotein, Alpha (B.1.1.7) S, Beta (B.1.351) S, Delta (B.1.617.2) S, or Omicron BA.1 (B.1.1.529) S using VeroE6 cells stably expressing TMPRSS2 (64, 67, 72, 73). G614 S VSV neutralization was significantly reduced upon depletion of RBD-directed antibodies and, to a lesser extent, after depletion of NTD-directed antibodies for all samples tested (Fig. 3B and fig. S13A). This suggests that both RBD- and NTD-targeting polyclonal plasma antibodies contribute to vaccine-elicited neutralizing activity of vaccine-matched Wuhan-Hu-1 SARS-CoV-2 pseudovirus [the D614G mutation has a very small effect on neutralization mediated by human plasma antibodies (74)]. Neutralization of the Alpha, Beta, Delta, and Omicron BA.1 S VSV pseudoviruses revealed a near-complete loss of neutralizing activity after depletion of RBD-directed plasma antibodies but no detectable contribution of NTD-directed antibodies (Fig. 3, C to F, and fig. S13, B to E). Because depletion of RBD-directed antibodies completely abrogated variant cross-neutralization, vaccine-elicited neutralization breadth is almost completely accounted for by antibodies targeting this domain. These data concur with (i) the marked antigenic variation of the SARS-CoV-2 NTD among variants and sarbecoviruses, which is associated with a narrow specificity of NTD neutralizing antibodies (25, 28, 66, 67, 73, 75), and (ii) the description of multiple broadly neutralizing sarbecovirus antibodies recognizing distinct RBD antigenic sites (14–16, 18, 76–82).

### DISCUSSION

The discovery that most neutralizing activity in individuals infected with respiratory syncytial virus targets prefusion F led to the subsequent stabilization of this conformational state through protein engineering and yielded clinically advanced vaccine candidates against this pathogen (69, 70, 85–88). We demonstrate here that prefusion SARS-CoV-2 S binding titers correlate with plasma neutralizing activity largely due to targeting of the S<sub>1</sub> subunit, which comprises antigenic sites recognized by most neutralizing antibodies and is shed upon refolding. Targeting of the S<sub>2</sub> subunit makes little contribution to vaccine-elicited polyclonal neutralizing activity due to the low frequency and weak potency of fusion machinery-directed neutralizing antibodies (30, 33–36, 89), although screening larger cohorts might help in identifying individuals with a greater proportion of S<sub>2</sub>-targeting neutralizing antibodies. The data presented here in humans concur with mouse and nonhuman primate immunogenicity studies showing that prefusion-stabilized 2P S glycoproteins elicit greater neutralizing antibody titers than nonstabilized S trimers (44, 48, 90). These outcomes are likely resulting from the metastability of prefusion S and suggest that engineering next-generation S immunogens with additional prefusion-stabilizing mutations [e.g., “HexaPro S” (91) or “VLFIP” S (92)] could lead to vaccines eliciting even greater neutralizing antibody titers and resilience to SARS-CoV-2 variants. The identification of the RBD as the sole target of vaccine-elicited polyclonal antibodies broadly neutralizing SARS-CoV-2 variants is reminiscent of recent reports describing broadly neutralizing sarbecovirus monoclonal antibodies isolated from infected individuals (14–16, 18, 20, 76–78, 93) and the rapid accumulations of mutations in the NTD (25, 66, 67, 73, 75). Although cross-variant plasma neutralization is determined by RBD-directed antibodies, we note that Fc-mediated effector functions, including antibody-dependent phagocytosis, cellular cytotoxicity, and complement activation, can play key roles for in vivo protection in addition to direct viral neutralization (94–99). These findings motivate the clinical development of RBD-based vaccines against SARS-CoV-2 (37, 100–104) and sarbecoviruses (105–108) for future pandemic preparedness.

### MATERIALS AND METHODS

#### Study design

To study the influence of the SARS-CoV-2 S conformation on plasma neutralizing activity, we collected human plasma samples from individuals who had received a primary vaccine series of the Moderna/NIAID mRNA-1273, Pfizer/BioNTech BNT162b2, Novavax NVX-CoV2373, AstraZeneca/Oxford AZD1222, Gamaleya Research Institute Sputnik V, Janssen Ad26.COVS.2, or Sinopharm BBIBP-CorV with or without administration of homologous or heterologous boosters and with or without prior SARS-CoV-2 exposure. To understand the molecular basis of elicitation of neutralizing antibodies, we assessed the specificity of S-directed antibody responses for various S constructs, the correlation between antibody binding titers and neutralization potency, and the relative contribution of the RBD and the NTD to vaccine-matched and vaccine-mismatched cross-neutralizing activity against SARS-CoV-2 variants.

## Cell lines

Cell lines used in this study were obtained from Thermo Fisher Scientific [human embryonic kidney (HEK) 293T and Expi293F] or were gifted by F. Lempp [Vero-TMPRSS2 cells (64)]. None of the cell lines used was authenticated or tested for mycoplasma contamination.

## Sample donors

Convalescent plasma, mRNA-1273, BNT162b2, and previously infected BNT162b2 and Ad26.COVS.S samples were obtained from the Hospitalized or Ambulatory Adults with Respiratory Viral Infections study approved by the University of Washington Human Subjects Division Institutional Review Board (IRB) (STUDY00000959). Some mRNA-1273 samples were obtained from individuals enrolled in the United World Antiviral Research Network (UWARN): COVID-19 in WA study approved by the University of Washington Human Subjects Division IRB (STUDY00010350). Samples from NVX-CoV2373-immunized individuals were collected in the San Diego region by the La Jolla Institute for Immunology (54). This work was approved by the IRB of the La Jolla Institute (IRB no. VD-214). Ad26.COVS.S samples were obtained from and approved by the Infectious Diseases Clinical Research Consortium. AZD1222 samples were obtained from the PolImmune-COVID study conducted by Istituto Nazionale Genetica Molecolare and Istituto di Ricovero e Cura a Carattere Scientifico Ca' Granda Ospedale Maggiore Policlinico di Milan, approved by Istituto Nazionale per le Malattie Infettive "Lazzaro Spallanzani" Ethics Committee (286\_2021). Sputnik V samples were obtained from health care workers at the Hospital de Clínicas "José de San Martín," Buenos Aires, Argentina. BBIBP-CorV samples were obtained from Aga Khan University, Karachi, Pakistan. Demographic data for these individuals are summarized in table S2.

## Plasmid construction

The SARS-CoV-2 S-6P is as previously described (91) and was placed into pCMV with an octa-his tag. The SARS-CoV-2 NTD (residues 14 to 307) with a C-terminal 8XHis-tag was subcloned in pCMV as previously described (25). The SARS-CoV-2-RBD-Avi construct was synthesized by GenScript into pcDNA3.1<sup>-</sup> with an N-terminal mu-phosphatase signal peptide and a C-terminal octa-histidine tag, flexible linker, and avi tag (GHHHHHHHHGGSSGLNDIFEAQKIEWHE). The boundaries of the construct are N<sub>-328</sub>RFPN<sub>331</sub> and <sub>528</sub>KKST<sub>531</sub>-C (1). SARS-CoV-2 S G614 (9) has a mu-phosphatase signal peptide beginning at Q14 and a mutated S1/S2 cleavage site (SGAR), ends at residue K1211, and is followed by a tobacco etch virus (TEV) cleavage site, fold-on trimerization motif, and an 8× His tag in the pCMV vector. SARS-CoV-2 S<sub>1</sub> has a mu-phosphatase signal peptide, mutated furin cleavage site to SGAS, D614G mutation, and Rpk9 mutations (Y365F/F392W/V395I) and ends at S686, followed by a 16GS linker, I53-50A, and C-terminal his tag. SARS-CoV-2 S<sub>2</sub> has a mu-phosphatase signal peptide and begins at <sup>686689</sup> with stabilizing mutations from the vFlip construct (Y707C/T883C, A892P, A899P, A942P, and V967P) (92). It also contains a F970C-G999C disulfide to further lock into the prefusion (C. Simmerling, personal communication). The construct ends at residue Q1208 and is followed by a fold-on trimerization motif, a TEV cleavage site, an 8× His tag, and an avi tag in the CMVR vector. SARS-CoV-2 G614 S (YP 009724390.1), Alpha (B.1.1.7), Beta (B.1.351), and Delta

(B.1.617.2) S genes were all placed into the HDM vector with a 21-residue C-terminal deletion as previously described (67, 105, 109). The plasmids encoding the SARS-CoV-2 Omicron BA.1 S variant were generated by overlapping polymerase chain reaction mutagenesis of the wild-type plasmid pcDNA3.1(+)-spike-D19 (110).

## Protein expression and purification

SARS-CoV-2 S subunits and domains were produced in Expi293F cells (Thermo Fisher Scientific) grown in suspension using Expi293 Expression Medium (Thermo Fisher Scientific) at 37°C in a humidified 8% CO<sub>2</sub> incubator rotating at 130 rpm. Cells grown to a density of 3 million cells/ml were transfected using the ExpiFectamine 293 Transfection Kit (Thermo Fisher Scientific) and cultivated for 3 to 5 days. Proteins were purified from clarified supernatants using a nickel HisTrap HP affinity column (Cytiva) and washed with 10 column volumes of 20 mM imidazole, 25 mM sodium phosphate (pH 8.0), and 300 mM NaCl before elution on a gradient to 500 mM imidazole. To produce SARS-CoV-2 S in the postfusion state, we incubated SARS-CoV-2 S D614G with 1:1 (w/w) S2X58-Fab (16) and trypsin (10 μg/ml) for 1 hour at 37°C before size exclusion on a Superose 6 Increase column (Cytiva). Proteins were buffer-exchanged into 20 mM sodium phosphate (pH 8) and 100 mM NaCl and concentrated using centrifugal filters (Amicon Ultra) before being flash-frozen.

## Antibody expression and purification

RAY-53-IgG (Huang *et al.* 2021) was produced in ExpiCHO cells (Thermo Fisher Scientific) grown in suspension using ExpiCHO Expression Medium (Thermo Fisher Scientific) at 37°C in a humidified 8% CO<sub>2</sub> incubator rotating at 130 rpm. Cells grown to a density of 6 million cells/ml were transfected using the ExpiFectamine CHO Transfection Kit (Thermo Fisher Scientific) and cultivated for 6 to 8 days. Proteins were purified from clarified supernatants using a Protein A affinity column (Cytiva) and washed with 10 column volumes of 20 mM sodium phosphate (pH 8.0) before elution with 0.1 M citric acid (pH 3) into 1 M tris-HCl (pH 9). Proteins were buffer-exchanged into 20 mM sodium phosphate (pH 8) and 100 mM NaCl and concentrated using centrifugal filters (Amicon Ultra) before being flash-frozen.

## Enzyme-linked immunosorbent assay

Thirty microliters of SARS-CoV-2 S, NTD, RBD, S<sub>1</sub>, S<sub>2(Pre)</sub>, or S<sub>2(Post)</sub> (3 μg/ml) diluted in phosphate-buffered saline (PBS) were incubated on a 384-well Nunc Maxisorp plate (Thermo Fisher Scientific, 464718) for 1 hour at 37°C. Plates were slapped dry before the addition of 80 μl of blocker casein in PBS (Thermo Fisher Scientific) and incubation for 1 hour at 37°C. Plates were slapped dry, and a 1:4 serial dilution of plasma in 30 μl of Tris-buffered saline and polysorbate 20 (TBST) was added and incubated for 1 hour at 37°C. Plates were slapped dry and washed four times with TBST using a BioTek plate washer, followed by the addition of In-vitrogen anti-human IgG (Thermo Fisher Scientific, A18817) and 1 hour of incubation at 37°C. Plates were once again slapped dry and washed four times with TBST before the addition of room temperature TMB Microwell Peroxidase (Seracare, 5120-0083). The reaction was quenched after 1 to 2 min with 1 N HCl, and the absorbance at 450 nm of each well was read using a BioTek plate



reader. Prism (GraphPad) area under the curve (AUC) was used to analyze data after log transformation of dilution series.

### Pseudotyped VSV production

SARS-CoV-2 G614, Alpha (B.1.1.7), Beta (B.1.351), Delta (B.1.617.2), and Omicron BA.1 pseudotypes were prepared similarly as previously described (67). Briefly, HEK293T cells seeded in poly-D-lysine-coated 100-mm dishes at ~75% confluency were washed five times with Opti-MEM and transfected using 24  $\mu\text{g}$  of the S glycoprotein plasmid with Lipofectamine 2000 (Life Technologies). After 5 hours at 37°C, media supplemented with 20% fetal bovine serum (FBS) and 2% penicillin G and streptomycin (Pen-Strep) was added. After 20 hours, cells were washed five times with Dulbecco's Modified Eagle Medium (DMEM), and cells were transduced with VSV $\Delta$ G-luc before a 2-hour incubation at 37°C. Infected cells were then washed an additional five times with DMEM before adding media supplemented with anti-VSV-G antibody [I1-mouse hybridoma supernatant diluted 1:25, from CRL-2700, American Type Culture Collection (ATCC)] to reduce parental background. After 18 to 24 hours, the supernatant was harvested and clarified by low-speed centrifugation at 2500g for 10 min. The supernatant was then filtered (0.45  $\mu\text{m}$ ) and concentrated 10 times using a 30-kDa molecular weight cutoff centrifugal concentrator (Amicon Ultra). The pseudotypes were then aliquoted and frozen at -80°C.

### Pseudotyped VSV neutralization assay

To evaluate neutralization of G614, Alpha (B.1.1.7), Beta (B.1.351), Delta (B.1.617.2), and Omicron BA.1 pseudotypes by the plasma of vaccinees or previously infected individuals, Vero-TMPRSS2 cells in DMEM supplemented with 10% FBS, 1% PenStrep, and puromycin (8  $\mu\text{g}/\text{ml}$ ) were seeded at 60 to 70% confluency into white clear-bottom 96-well plates (Corning) and incubated at 37°C. The following day, a half-area 96-well plate (Greiner) was prepared with eight threefold serial plasma dilutions. An equal volume of DMEM with 1:25 pseudovirus and 1:25 anti-VSV-G antibody (I1-mouse hybridoma supernatant from CRL-2700, ATCC) was then added to the half-area plate. The mixture was incubated at room temperature for 20 to 30 min. Media were removed from the cells, and 40  $\mu\text{l}$  from each well (containing plasma and pseudovirus) were transferred to the 96-well plate seeded with Vero-TMPRESS2 cells and incubated at 37°C for 2 hours. After 2 hours, an additional 40  $\mu\text{l}$  of DMEM supplemented with 20% FBS and 2% PenStrep was added to the cells. After 16 to 20 hours, 40  $\mu\text{l}$  of One-Glo-EX substrate (Promega) were added to each well and incubated on a plate shaker in the dark for 5 min. Relative luciferase units were read using a BioTek plate reader. Relative luciferase units were plotted and normalized in Prism (GraphPad): 100% neutralization being cells lacking pseudovirus and 0% neutralizing being cells containing virus but lacking plasma. Prism (GraphPad) nonlinear regression with "[inhibitor] versus normalized response with a variable slope" was used to determine median inhibitory dose values from curve fits with two or three repeats. Two to four biological replicates were carried out for each sample.

### Depletion of SARS-CoV-2 S-binding antibodies from polyclonal plasma

Vortexed Invitrogen His-Tag Dynabeads (400  $\mu\text{l}$ ; Thermo Fisher Scientific, 10104D) were aliquoted into microcentrifuge tubes and

incubated on an Invitrogen DynaMag-2 Magnet (Thermo Fisher Scientific, 12-321-D) for 2 min. The supernatant was discarded, and beads were washed with 300  $\mu\text{l}$  of TBST. After a 2-min incubation on the magnet, the supernatant was discarded, and 100  $\mu\text{g}$  of his-tagged S, S<sub>1</sub>, S<sub>2(Pre)</sub>, S<sub>2(Post)</sub>, NTD, or RBD in 300  $\mu\text{l}$  of TBST were left to incubate with the beads for 10 to 20 min at room temperature. The magnet was used, and the supernatant was discarded. The beads were spun down and put on the magnet, and excess liquid was removed before the addition of 15 to 20  $\mu\text{l}$  of the plasma of interest. The plasma was left to incubate at room temperature with the beads for 20 to 30 min before being removed.

### Negative stain EM sample preparation and data collection

Protein samples were diluted to 0.01 mg/ml immediately before adsorption to glow-discharged carbon-coated copper grids for ~30 s before a 2% uranyl formate staining. Micrographs were recorded using the Legikon software on a 120 kV FEI Tecnai G2 Spirit with a Gatan Ultrascan 4000 4k  $\times$  4k charge-coupled device camera at  $\times$ 67,000 nominal magnification. The defocus ranged from -1.0 to -2.0  $\mu\text{m}$ , and the pixel size was 1.6  $\text{\AA}$ .

### CryoEM sample preparation, data collection, and data processing

Three microliters of the recombinantly expressed and purified prefusion SARS-CoV-2 S<sub>2</sub> subunit were loaded onto freshly glow-discharged R 2/2 UltrAuFoil grids (200 mesh) (111) before plunge-freezing using a vitrobot MarkIV (Thermo Fisher Scientific) with a blot force of 0 and blot time of 6.5 s at 100% humidity and 22°C. Data were acquired using an FEI Titan Krios transmission electron microscope operated at 300 kV and equipped with a Gatan K3 direct detector and Gatan Quantum GIF energy filter, operated in zero-loss mode with a slit width of 20 eV. Automated data collection was carried out using Legikon (112) at a nominal magnification of  $\times$ 105,000 with a physical pixel size of 0.843  $\text{\AA}$ . The dose rate was adjusted to 15 counts/pixel per second, and each movie was acquired in superresolution mode fractionated in 75 frames of 40 ms. Micrographs (7859) were collected with a defocus range between -0.5 and -2.5  $\mu\text{m}$ . Movie frame alignment, estimation of the microscope contrast-transfer function parameters, particle picking, and extraction were carried out using Warp (113).

Two rounds of reference-free two-dimensional (2D) classification were performed using CryoSPARC (114) to select well-defined particle images. These selected particles were subjected to two rounds of 3D classification with 50 iterations each (angular sampling of 7.5° for 25 iterations and 1.8° with local search for 25 iterations), using an ab initio map as initial model, in Relion (115). 3D refinements were carried out using nonuniform refinement along with per-particle defocus refinement in CryoSPARC (116). We subjected selected particle images to the Bayesian polishing procedure (117) implemented in Relion 3.0 before performing another round of nonuniform refinement in cryoSPARC followed by per-particle defocus refinement and again nonuniform refinement. Local resolution estimation, filtering, and sharpening were carried out using CryoSPARC. Reported resolutions are based on the gold-standard Fourier shell correlation of 0.143 criterion, and Fourier shell correlation curves were corrected for the effects of soft masking by high-resolution noise substitution (118, 119).

## Model building and refinement

UCSF Chimera (120) and Coot (121) were used to fit and rebuild an atomic model derived from Protein Data Bank (PDB) 6VXX (1) into the cryoEM map. The model was subsequently refined and relaxed with Rosetta using sharpened and unsharpened maps (122, 123). Model validation and analysis used MolProbity (124), EMringer (125), Phenix (126), and Privateer (127). Figures were generated using UCSF Chimera X (128).

## Statistical analysis

Statistical significance analysis of differences between binding titers of the same antigen or neutralization titers, after immunization with different vaccines, was determined using Tukey's multiple comparisons test. Statistical significance analysis of differences between binding titers of different antigens, after immunization with the same vaccine, was determined using paired Tukey's multiple comparisons test. Statistical significance analysis of differences between mock and depleted samples was determined using ratio paired Wilcoxon rank test.

## Supplementary Materials

This PDF file includes:

Figs S1 to S13  
Tables S1 to S9

Other Supplementary Material for this manuscript includes the following:

MDAR Reproducibility Checklist  
Data S1

[View/request a protocol for this paper from Bio-protocol.](#)

## REFERENCES AND NOTES

1. A. C. Walls, Y.-J. Park, M. A. Tortorici, A. Wall, A. T. McGuire, D. Veelsler, Structure, function, and antigenicity of the SARS-CoV-2 spike glycoprotein. *Cell* **181**, 281–292.e6 (2020).
2. D. Wrapp, N. Wang, K. S. Corbett, J. A. Goldsmith, C. L. Hsieh, O. Abiona, B. S. Graham, J. S. McLellan, Cryo-EM structure of the 2019-nCoV spike in the prefusion conformation. *Science* **367**, 1260–1263 (2020).
3. M. Hoffmann, H. Kleine-Weber, S. Schroeder, N. Krüger, T. Herrler, S. Erichsen, T. S. Schiergens, G. Herrler, N. H. Wu, A. Nitsche, M. A. Müller, C. Drosten, S. Pöhlmann, SARS-CoV-2 cell entry depends on ACE2 and TMPRSS2 and is blocked by a clinically proven protease inhibitor. *Cell* **181**, 271–280.e8 (2020).
4. M. Hoffmann, H. Kleine-Weber, S. Pöhlmann, A multibasic cleavage site in the spike protein of SARS-CoV-2 is essential for infection of human lung cells. *Mol. Cell* **78**, 779–784.e5 (2020).
5. M. Letko, A. Marzi, V. Munster, Functional assessment of cell entry and receptor usage for SARS-CoV-2 and other lineage B betacoronaviruses. *Nat. Microbiol.* **5**, 562–569 (2020).
6. P. Zhou, X.-L. Yang, X.-G. Wang, B. Hu, L. Zhang, W. Zhang, H.-R. Si, Y. Zhu, B. Li, C.-L. Huang, H.-D. Chen, J. Chen, Y. Luo, H. Guo, R.-D. Jiang, M.-Q. Liu, Y. Chen, X.-R. Shen, X. Wang, X.-S. Zheng, K. Zhao, Q.-J. Chen, F. Deng, L.-L. Liu, B. Yan, F.-X. Zhan, Y.-Y. Wang, G.-F. Xiao, Z.-L. Shi, A pneumonia outbreak associated with a new coronavirus of probable bat origin. *Nature* **579**, 270–273 (2020).
7. M. McCallum, N. Czudnochowski, L. E. Rosen, S. K. Zepeda, J. E. Bowen, A. C. Walls, K. Hauser, A. Joshi, C. Stewart, J. R. Dillen, A. E. Powell, T. I. Croll, J. Nix, H. W. Virgin, D. Corti, G. Snell, D. Veelsler, Structural basis of SARS-CoV-2 omicron immune evasion and receptor engagement. *Science* **375**, 864–868 (2022).
8. S. Wang, Z. Qiu, Y. Hou, X. Deng, W. Xu, T. Zheng, P. Wu, S. Xie, W. Bian, C. Zhang, Z. Sun, K. Liu, C. Shan, A. Lin, S. Jiang, Y. Xie, Q. Zhou, L. Lu, J. Huang, X. Li, AXL is a candidate receptor for SARS-CoV-2 that promotes infection of pulmonary and bronchial epithelial cells. *Cell Res.* **31**, 126–140 (2021).
9. F. A. Lempp, L. Soriaga, M. Montiel-Ruiz, F. Benigni, J. Noack, Y.-J. Park, S. Bianchi, A. C. Walls, J. E. Bowen, J. Zhou, H. Kaiser, M. Agostini, M. Meury, E. Dellota Jr, S. Jaconi, E. Camerani, H. W. Virgin, A. Lanzavecchia, D. Veelsler, L. Purcell, A. Telenti, D. Corti, Membrane lectins enhance SARS-CoV-2 infection and influence the neutralizing activity of different classes of antibodies. *bioRxiv* 10.1101/2021.04.03.438258 (2021).
10. W. T. Soh, Y. Liu, E. E. Nakayama, C. Ono, S. Torii, H. Nakagami, Y. Matsuura, T. Shioda, H. Arase, The N-terminal domain of spike glycoprotein mediates SARS-CoV-2 infection by associating with L-SIGN and DC-SIGN. *bioRxiv* 10.1101/2020.11.05.369264 (2020).
11. A. C. Walls, M. A. Tortorici, J. Snijder, X. Xiong, B. J. Bosch, F. A. Rey, D. Veelsler, Tectonic conformational changes of a coronavirus spike glycoprotein promote membrane fusion. *Proc. Natl. Acad. Sci. U.S.A.* **114**, 11157–11162 (2017).
12. Y. Cai, J. Zhang, T. Xiao, H. Peng, S. M. Sterling, R. M. Walsh Jr., S. Rawson, S. Rits-Volloch, B. Chen, Distinct conformational states of SARS-CoV-2 spike protein. *Science* **369**, 1586–1592 (2020).
13. A. C. Walls, M. A. Tortorici, B. J. Bosch, B. Frenz, P. J. M. Rottier, F. DiMaio, F. A. Rey, D. Veelsler, Cryo-electron microscopy structure of a coronavirus spike glycoprotein trimer. *Nature* **531**, 114–117 (2016).
14. D. Pinto, Y. J. Park, M. Beltramello, A. C. Walls, M. A. Tortorici, S. Bianchi, S. Jaconi, K. Culap, F. Zatta, A. De Marco, A. Peter, B. Guarino, R. Spreafico, E. Camerani, J. B. Case, R. E. Chen, C. Havenar-Daughton, G. Snell, A. Telenti, H. W. Virgin, A. Lanzavecchia, M. S. Diamond, K. Fink, D. Veelsler, D. Corti, Cross-neutralization of SARS-CoV-2 by a human monoclonal SARS-CoV antibody. *Nature* **583**, 290–295 (2020).
15. M. A. Tortorici, N. Czudnochowski, T. N. Starr, R. Marzi, A. C. Walls, F. Zatta, J. E. Bowen, S. Jaconi, J. Di Iulio, Z. Wang, A. De Marco, S. K. Zepeda, D. Pinto, Z. Liu, M. Beltramello, I. Bartha, M. P. Housley, F. A. Lempp, L. E. Rosen, E. Dellota Jr., H. Kaiser, M. Montiel-Ruiz, J. Zhou, A. Addetia, B. Guarino, K. Culap, N. Sprugasci, C. Saliba, E. Vetti, I. Giacchetto-Sasselli, C. S. Fregni, R. Abdelnabi, S.-Y. C. Foo, C. Havenar-Daughton, M. A. Schmid, F. Benigni, E. Camerani, J. Neyts, A. Telenti, H. W. Virgin, S. P. J. Whelan, G. Snell, J. D. Bloom, D. Corti, D. Veelsler, M. S. Pizzuto, Broad sarbecovirus neutralization by a human monoclonal antibody. *Nature* **597**, 103–108 (2021).
16. T. N. Starr, N. Czudnochowski, Z. Liu, F. Zatta, Y.-J. Park, A. Addetia, D. Pinto, M. Beltramello, P. Hernandez, A. J. Greaney, R. Marzi, W. G. Glass, I. Zhang, A. S. Dingens, J. E. Bowen, M. A. Tortorici, A. C. Walls, J. A. Wojcechowskyj, A. De Marco, L. E. Rosen, J. Zhou, M. Montiel-Ruiz, H. Kaiser, J. Dillen, H. Tucker, J. Bassi, C. Silacci-Fregni, M. P. Housley, J. di Iulio, G. Lombardo, M. Agostini, N. Sprugasci, K. Culap, S. Jaconi, M. Meury, E. Dellota, R. Abdelnabi, S.-Y. C. Foo, E. Camerani, S. Stumpf, T. I. Croll, J. C. Nix, C. Havenar-Daughton, L. Piccoli, F. Benigni, J. Neyts, A. Telenti, F. A. Lempp, M. S. Pizzuto, J. D. Chodera, C. M. Hebner, H. W. Virgin, S. P. J. Whelan, D. Veelsler, D. Corti, J. D. Bloom, G. Snell, SARS-CoV-2 RBD antibodies that maximize breadth and resistance to escape. *Nature* **597**, 97–102 (2021).
17. L. Piccoli, Y. J. Park, M. A. Tortorici, N. Czudnochowski, A. C. Walls, M. Beltramello, C. Silacci-Fregni, D. Pinto, L. E. Rosen, J. E. Bowen, O. J. Acton, S. Jaconi, B. Guarino, A. Minola, F. Zatta, N. Sprugasci, J. Bassi, A. Peter, A. De Marco, J. C. Nix, F. Mele, S. Jovic, B. F. Rodriguez, S. V. Gupta, F. Jin, G. Piumatti, G. Lo Presti, A. F. Pellanda, M. Biggiogero, M. Tarkowski, M. S. Pizzuto, E. Camerani, C. Havenar-Daughton, M. Smithey, D. Hong, V. Lepori, E. Albanese, A. Ceschi, E. Bernasconi, L. Elzi, P. Ferrari, C. Garzoni, A. Riva, G. Snell, F. Sallusto, K. Fink, H. W. Virgin, A. Lanzavecchia, D. Corti, D. Veelsler, Mapping neutralizing and immunodominant sites on the SARS-CoV-2 spike receptor-binding domain by structure-guided high-resolution serology. *Cell* **183**, 1024–1042.e21 (2020).
18. M. A. Tortorici, M. Beltramello, F. A. Lempp, D. Pinto, H. V. Dang, L. E. Rosen, M. McCallum, J. Bowen, A. Minola, S. Jaconi, F. Zatta, A. De Marco, B. Guarino, S. Bianchi, E. J. Lauron, H. Tucker, J. Zhou, A. Peter, C. Havenar-Daughton, J. A. Wojcechowskyj, J. B. Case, R. E. Chen, H. Kaiser, M. Montiel-Ruiz, M. Meury, N. Czudnochowski, R. Spreafico, J. Dillen, C. Ng, N. Sprugasci, K. Culap, F. Benigni, R. Abdelnabi, S. C. Foo, M. A. Schmid, E. Camerani, A. Riva, A. Gabrieli, M. Galli, M. S. Pizzuto, J. Neyts, M. S. Diamond, H. W. Virgin, G. Snell, D. Corti, K. Fink, D. Veelsler, Ultrapotent human antibodies protect against SARS-CoV-2 challenge via multiple mechanisms. *Science* **370**, 950–957 (2020).
19. B. E. Jones, P. L. Brown-Augsburger, K. S. Corbett, K. Westendorf, J. Davies, T. P. Cujec, C. M. Wiethoff, J. L. Blackburn, B. A. Heinz, D. Foster, R. E. Higgs, D. Balasubramaniam, L. Wang, Y. Zhang, E. S. Yang, R. Bidshahri, L. Kraft, Y. Hwang, S. Zentelis, K. R. Jepsen, R. Goya, M. A. Smith, D. W. Collins, S. J. Hinshaw, S. A. Tycho, D. Pellacani, P. Xiang, K. Muthuraman, S. Sobhanifar, M. H. Piper, F. J. Triana, J. Hendle, A. Pustilnik, A. C. Adams, S. J. Berens, R. S. Baric, D. R. Martinez, R. W. Cross, T. W. Geisbert, V. Borisovich, O. Abiona, H. M. Belli, M. de Vries, A. Mohamed, M. Dittmann, M. I. Samanovic, M. J. Mulligan, J. A. Goldsmith, C.-L. Hsieh, N. V. Johnson, D. Wrapp, J. S. McLellan, B. C. Barnhart, B. S. Graham, J. R. Mascola, C. L. Hansen, E. Falconer, The neutralizing antibody, LY-CoV555, protects against SARS-CoV-2 infection in nonhuman primates. *Sci. Transl. Med.* **13**, eabf1906 (2021).
20. C. A. Jette, A. A. Cohen, P. N. P. Gnanaprasagam, F. Muecksch, Y. E. Lee, K. E. Huey-Tubman, F. Schmidt, T. Hatziioannou, P. D. Bieniasz, M. C. Nussenzweig, A. P. West, J. R. Keeffe, P. J. Bjorkman, C. O. Barnes, Broad cross-reactivity across sarbecoviruses exhibited by a subset of COVID-19 donor-derived neutralizing antibodies. *Cell Rep.* **37**, 110188 (2021).

21. C. O. Barnes, C. A. Jette, M. E. Abernathy, K.-M. A. Dam, S. R. Esswein, H. B. Grinstead, A. G. Malyutin, N. G. Sharaf, K. E. Huey-Tubman, Y. E. Lee, D. F. Robbiani, M. C. Nussenzweig, A. P. West Jr., P. J. Bjorkman, SARS-CoV-2 neutralizing antibody structures inform therapeutic strategies. *Nature* **588**, 682–687 (2020).
22. J. Dong, S. J. Zost, A. J. Greaney, T. N. Starr, A. S. Dingens, E. C. Chen, R. E. Chen, J. B. Case, R. E. Sutton, P. Gilchuk, J. Rodriguez, E. Armstrong, C. Gainza, R. S. Nargi, E. Binshtein, X. Xie, X. Zhang, P.-Y. Shi, J. Logue, S. Weston, M. E. McGrath, M. B. Frieman, T. Brady, K. M. Tuffy, H. Bright, Y.-M. Loo, P. M. McTamney, M. T. Esser, R. H. Carnahan, M. S. Diamond, J. D. Bloom, J. E. Crowe Jr., Genetic and structural basis for SARS-CoV-2 variant neutralization by a two-antibody cocktail. *Nat. Microbiol.* **6**, 1233–1244 (2021).
23. S. J. Zost, P. Gilchuk, J. B. Case, E. Binshtein, R. E. Chen, J. P. Nkolola, A. Schäfer, J. X. Reidy, A. Trivette, R. S. Nargi, R. E. Sutton, N. Suryadevara, D. R. Martinez, L. E. Williamson, E. C. Chen, T. Jones, S. Day, L. Myers, A. O. Hassan, N. M. Kafai, E. S. Winkler, J. M. Fox, S. Shrihari, B. K. Mueller, J. Meiler, A. Chandrashekar, N. B. Mercado, J. J. Steinhart, K. Ren, Y. M. Loo, N. L. Kallewaard, B. L. McCune, S. P. Keeler, M. B. Frieman, D. H. Barouch, L. E. Gralinski, R. S. Baric, L. B. Thackray, M. S. Diamond, R. H. Carnahan, J. E. Crowe Jr., Potently neutralizing and protective human antibodies against SARS-CoV-2. *Nature* **584**, 443–449 (2020).
24. C. Wang, W. Li, D. Drabek, N. M. A. Okba, R. van Haperen, A. D. M. E. Osterhaus, F. J. M. van Kuppeveld, B. L. Haagmans, F. Grosveld, B. J. Bosch, A human monoclonal antibody blocking SARS-CoV-2 infection. *Nat. Commun.* **11**, 2251 (2020).
25. M. McCallum, A. De Marco, F. A. Lempp, M. A. Tortorici, D. Pinto, A. C. Walls, M. Beltramello, A. Chen, Z. Liu, F. Zatta, S. Zepeda, J. di Iulio, J. E. Bowen, M. Montiel-Ruiz, J. Zhou, L. E. Rosen, S. Bianchi, B. Guarino, C. S. Fregni, R. Abdelnabi, S.-Y. Caroline Foo, P. W. Rothlauf, L.-M. Bloyet, F. Benigni, E. Camerani, J. Neyts, A. Riva, G. Snell, A. Telenti, S. P. J. Whelan, H. W. Virgin, D. Corti, M. S. Pizzuto, D. Velesler, N-terminal domain antigenic mapping reveals a site of vulnerability for SARS-CoV-2. *Cell* **184**, 2332–2347.e16 (2021).
26. G. Cerutti, Y. Guo, T. Zhou, J. Gorman, M. Lee, M. Rapp, E. R. Reddell, J. Yu, F. Bahna, J. Bimela, Y. Huang, P. S. Katsamba, L. Liu, M. S. Nair, R. Rawi, A. S. Ollia, P. Wang, B. Zhang, G.-Y. Chuang, D. D. Ho, Z. Sheng, P. D. Kwong, L. Shapiro, Potent SARS-CoV-2 neutralizing antibodies directed against spike N-terminal domain target a single supersite. *Cell Host Microbe* **29**, 819–833.e7 (2021).
27. X. Chi, R. Yan, J. Zhang, G. Zhang, Y. Zhang, M. Hao, Z. Zhang, P. Fan, Y. Dong, Y. Yang, Z. Chen, Y. Guo, Y. Li, X. Song, Y. Chen, L. Xia, L. Fu, L. Hou, J. Xu, C. Yu, J. Li, Q. Zhou, W. Chen, A neutralizing human antibody binds to the N-terminal domain of the Spike protein of SARS-CoV-2. *Science* **369**, 650–655 (2020).
28. N. Suryadevara, S. Shrihari, P. Gilchuk, L. A. VanBlargan, E. Binshtein, S. J. Zost, R. S. Nargi, R. E. Sutton, E. S. Winkler, E. C. Chen, M. E. Fouch, E. Davidson, B. J. Doranz, R. E. Chen, P.-Y. Shi, R. H. Carnahan, L. B. Thackray, M. S. Diamond, J. E. Crowe Jr., Neutralizing and protective human monoclonal antibodies recognizing the N-terminal domain of the SARS-CoV-2 spike protein. *Cell* **184**, 2316–2331.e15 (2021).
29. Z. Wang, F. Muecksch, A. Cho, C. Gaebler, H.-H. Hoffmann, V. Ramos, S. Zong, M. Cipolla, B. Johnson, F. Schmidt, J. DaSilva, E. Bednarski, T. Ben Tanfous, R. Raspe, K. Yao, Y. E. Lee, T. Chen, M. Turroja, K. G. Milard, J. Dizon, A. Kaczynska, A. Gazumyan, T. Y. Oliveira, C. M. Rice, M. Caskey, P. D. Bieniasz, T. Hatziioannou, C. O. Barnes, M. C. Nussenzweig, Analysis of memory B cells identifies conserved neutralizing epitopes on the N-terminal domain of variant SARS-CoV-2 spike proteins. *Immunity* **55**, 998–1012.e8 (2022).
30. M. M. Sauer, M. A. Tortorici, Y.-J. Park, A. C. Walls, L. Homad, O. J. Acton, J. E. Bowen, C. Wang, X. Xiong, W. de van der Schueren, J. Quispe, B. G. Hoffstrom, B.-J. Bosch, A. T. McGuire, D. Velesler, Structural basis for broad coronavirus neutralization. *Nat. Struct. Mol. Biol.* **28**, 478–486 (2021).
31. C. Wang, R. van Haperen, J. Gutiérrez-Álvarez, W. Li, N. M. A. Okba, I. Albuлесcu, I. Widjaja, B. van Dieren, R. Fernandez-Delgado, I. Sola, D. L. Hurdiss, O. Daramola, F. Grosveld, F. J. M. van Kuppeveld, B. L. Haagmans, L. Enjuanes, D. Drabek, B.-J. Bosch, A conserved immunogenic and vulnerable site on the coronavirus spike protein delineated by cross-reactive monoclonal antibodies. *Nat. Commun.* **12**, 1715 (2021).
32. P. Zhou, M. Yuan, G. Song, N. Beutler, N. Shaabani, D. Huang, W.-T. He, X. Zhu, S. Callaghan, P. Yong, F. Anzanello, L. Peng, J. Ricketts, M. Parren, E. Garcia, S. A. Rawlings, D. M. Smith, D. Nemazee, J. R. Teijaro, T. F. Rogers, I. A. Wilson, D. R. Burton, R. Andrabi, A human antibody reveals a conserved site on beta-coronavirus spike proteins and confers protection against SARS-CoV-2 infection. *Sci. Transl. Med.* **eabi9215** (2021).
33. D. Pinto, M. M. Sauer, N. Czudnochowski, J. S. Low, M. Alejandra Tortorici, M. P. Housley, J. Noack, A. C. Walls, J. E. Bowen, B. Guarino, L. E. Rosen, J. di Iulio, J. Jerak, H. Kaiser, S. Islam, S. Jaconi, N. Sprugasci, K. Culap, R. Abdelnabi, C. Foo, L. Coelmont, I. Bartha, S. Bianchi, C. Silacci-Fregni, J. Bassi, R. Marzi, E. Vetti, A. Cassotta, A. Ceschi, P. Ferrari, P. E. Cippà, O. Giannini, S. Ceruti, C. Garzoni, A. Riva, F. Benigni, E. Camerani, L. Piccoli, M. S. Pizzuto, M. Smidhey, D. Hong, A. Telenti, F. A. Lempp, J. Neyts, C. Havenar-Daughton, A. Lanzavecchia, F. Sallusto, G. Snell, H. W. Virgin, M. Beltramello, D. Corti, D. Velesler, Broad betacoronavirus neutralization by a stem helix-specific human antibody. *Science* **373**, 1109–1116 (2021).
34. J. S. Low, J. Jerak, M. A. Tortorici, M. McCallum, D. Pinto, A. Cassotta, M. Foglierini, F. Mele, R. Abdelnabi, B. Weyand, J. Noack, M. Montiel-Ruiz, S. Bianchi, F. Benigni, N. Sprugasci, A. Joshi, J. E. Bowen, C. Stewart, M. Rexhepaj, A. C. Walls, D. Jarrossay, D. Morone, P. Paparoditis, C. Garzoni, P. Ferrari, A. Ceschi, J. Neyts, L. A. Purcell, G. Snell, D. Corti, A. Lanzavecchia, D. Velesler, F. Sallusto, ACE2-binding exposes the SARS-CoV-2 fusion peptide to broadly neutralizing coronavirus antibodies. *Science* **377**, eabq2679 (2022).
35. G. Song, W.-T. He, S. Callaghan, F. Anzanello, D. Huang, J. Ricketts, J. L. Torres, N. Beutler, L. Peng, S. Vargas, J. Cassell, M. Parren, L. Yang, C. Ignacio, D. M. Smith, J. E. Voss, D. Nemazee, A. B. Ward, T. Rogers, D. R. Burton, R. Andrabi, Cross-reactive serum and memory B-cell responses to spike protein in SARS-CoV-2 and endemic coronavirus infection. *Nat. Commun.* **12**, 2938 (2021).
36. Y. Huang, A. W. Nguyen, C.-L. Hsieh, R. Silva, O. S. Olaluwoye, R. E. Wilen, T. S. Kaoud, L. R. Azouz, A. N. Qerqez, K. C. Le, A. L. Bohanon, A. M. DiVenere, Y. Liu, A. G. Lee, D. Amengor, K. N. Dalby, S. D'Arcy, J. S. McLellan, J. A. Maynard, Identification of a conserved neutralizing epitope present on spike proteins from all highly pathogenic coronaviruses. *bioRxiv* 2021.01.31.428824 (2021). <https://doi.org/10.1101/2021.01.31.428824>.
37. P. S. Arunachalam, A. C. Walls, N. Golden, C. Atyeo, S. Fischinger, C. Li, P. Aye, M. J. Navarro, L. Lai, V. V. Edara, K. Röltgen, K. Rogers, L. Shirreff, D. E. Ferrell, S. Wrenn, D. Pettie, J. C. Kraft, M. C. Miranda, E. Kepl, C. Sydeman, N. Brunette, M. Murphy, B. Fiala, L. Carter, A. G. White, M. Trisal, C.-L. Hsieh, K. Russell-Lodrigue, C. Monjure, J. Dufour, S. Spencer, L. Doyle-Meyer, R. P. Bohm, N. J. Maness, C. Roy, J. A. Plante, K. S. Plante, A. Zhu, M. J. Gorman, S. Shin, X. Shen, J. Fontenot, S. Gupta, D. T. O'Hagan, R. Van Der Most, R. Rappuoli, R. L. Coffman, D. Novack, J. S. McLellan, S. Subramaniam, D. Montefiori, S. D. Boyd, J. L. Flynn, G. Alter, F. Villinger, H. Kleanthous, J. Rappaport, M. S. Suthar, N. P. King, D. Velesler, B. Pulendran, Adjuvanting a subunit COVID-19 vaccine to induce protective immunity. *Nature* **594**, 253–258 (2021).
38. K. McMahan, J. Yu, N. B. Mercado, C. Loos, L. H. Tostanoski, A. Chandrashekar, J. Liu, L. Peter, C. Atyeo, A. Zhu, E. A. Bondzie, G. Dagotto, M. S. Gebre, C. Jacob-Dolan, Z. Li, F. Nampanya, S. Patel, L. Pessaint, A. Van Ry, K. Blade, J. Yalley-Ogunro, M. Cabus, R. Brown, A. Cook, E. Teow, H. Andersen, M. G. Lewis, D. A. Lauffenburger, G. Alter, D. H. Barouch, Correlates of protection against SARS-CoV-2 in rhesus macaques. *Nature* **590**, 630–634 (2021).
39. D. S. Khoury, D. Cromer, A. Reynaldi, T. E. Schlub, A. K. Wheatley, J. A. Juno, K. Subbarao, S. J. Kent, J. A. Triccas, M. P. Davenport, Neutralizing antibody levels are highly predictive of immune protection from symptomatic SARS-CoV-2 infection. *Nat. Med.* **27**, 1205–1211 (2021).
40. K. S. Corbett, M. C. Nason, B. Flach, M. Gagne, S. O'Connell, T. S. Johnston, S. N. Shah, V. V. Edara, K. Floyd, L. Lai, C. McDanal, J. R. Francica, B. Flynn, K. Wu, A. Choi, M. Koch, O. M. Abiona, A. P. Werner, J. I. Molina, S. F. Andrew, M. M. Donaldson, J. Fintzi, D. R. Flebbe, E. Lamb, A. T. Noe, S. T. Nurmukhambetova, S. J. Provost, A. Cook, A. Dodson, A. Faudree, J. Greenhouse, S. Kar, L. Pessaint, M. Porto, K. Steingrebe, D. Valentin, S. Zouantcha, K. W. Bock, M. Minai, B. M. Nagata, R. van de Wetering, S. Boyoglu-Barnum, K. Leung, W. Shi, E. S. Yang, Y. Zhang, J.-P. M. Todd, L. Wang, G. S. Alvarado, H. Andersen, K. E. Foulds, D. K. Edwards, J. R. Mascola, I. N. Moore, M. G. Lewis, A. Carfi, D. Montefiori, M. S. Suthar, A. McDermott, M. Roederer, N. J. Sullivan, D. C. Douek, B. S. Graham, R. A. Seder, Immune correlates of protection by mRNA-1273 vaccine against SARS-CoV-2 in nonhuman primates. *Science* **373**, eabj0299 (2021).
41. P. B. Gilbert, D. C. Montefiori, A. B. McDermott, Y. Fong, D. Benkeser, W. Deng, H. Zhou, C. R. Houchens, K. Martins, L. Jayashankar, F. Castellino, B. Flach, B. C. Lin, S. O'Connell, C. McDanal, A. Eaton, M. Sarzotti-Kelsoe, Y. Lu, C. Yu, B. Borate, L. W. P. van der Laan, N. S. Hejazi, C. Huynh, J. Miller, H. M. El Sahly, L. R. Baden, M. Baron, L. De La Cruz, C. Gay, S. Kalam, C. F. Kelley, M. P. Andrasik, J. G. Kublin, L. Corey, K. M. Neuzil, L. N. Carpp, R. Pajon, D. Follmann, R. O. Donis, R. A. Koup; Immune Assays Team; Moderna, Inc. Team; Coronavirus Vaccine Prevention Network (CoVNP)/Coronavirus Efficacy (COVE) Team; United States Government (USG)/CoVNP Biostatistics Team, Immune correlates analysis of the mRNA-1273 COVID-19 vaccine efficacy clinical trial. *Science* **375**, 43–50 (2021).
42. D. Corti, L. A. Purcell, G. Snell, D. Velesler, Tackling COVID-19 with neutralizing monoclonal antibodies. *Cell* **184**, 3086–3108 (2021).
43. P. S. Arunachalam, Y. Feng, U. Ashraf, M. Hu, V. V. Edara, V. I. Zarnitsyna, P. P. Aye, N. Golden, K. W. M. Green, B. M. Threton, N. J. Maness, B. J. Beddingfield, R. P. Bohm, J. Dufour, K. Russell-Lodrigue, M. C. Miranda, A. C. Walls, K. Rogers, L. Shirreff, D. E. Ferrell, N. R. D. Adhikary, J. Fontenot, A. Grifoni, A. Sette, D. T. O'Hagan, R. Van Der Most, R. Rappuoli, F. Villinger, H. Kleanthous, J. Rappaport, M. S. Suthar, D. Velesler, T. T. Wang, N. P. King, B. Pulendran, Durable protection against SARS-CoV-2 Omicron variant is induced by an adjuvanted subunit vaccine. *Sci. Transl. Med.* **14**, eabq4130 (2022).
44. J. Pallesen, N. Wang, K. S. Corbett, D. Wrapp, R. N. Kirchdoerfer, H. L. Turner, C. A. Cottrell, M. M. Becker, L. Wang, W. Shi, W. P. Kong, E. L. Andres, A. N. Kettenbach, M. R. Denison, J. D. Chappell, B. S. Graham, A. B. Ward, J. S. McLellan, Immunogenicity and structures of a rationally designed prefusion MERS-CoV spike antigen. *Proc. Natl. Acad. Sci. U.S.A.* **114**, E7348–E7357 (2017).

45. K. S. Corbett, D. K. Edwards, S. R. Leist, O. M. Abiona, S. Boyoglu-Barnum, R. A. Gillespie, S. Himansu, A. Schäfer, C. T. Ziwawo, A. T. DiPiazza, K. H. Dinnon, S. M. Elbashir, C. A. Shaw, A. Woods, E. J. Fritch, D. R. Martinez, K. W. Bock, M. Minai, B. M. Nagata, G. B. Hutchinson, K. Wu, C. Henry, K. Bahl, D. Garcia-Dominguez, L. Ma, I. Renzi, W. P. Kong, S. D. Schmidt, L. Wang, Y. Zhang, E. Phung, L. A. Chang, R. J. Loomis, N. E. Altaras, E. Narayanan, M. Metkar, V. Presnyak, C. Liu, M. K. Louder, W. Shi, K. Leung, E. S. Yang, A. West, K. L. Gully, L. J. Stevens, N. Wang, D. Wrapp, N. A. Doria-Rose, G. Stewart-Jones, H. Bennett, G. S. Alvarado, M. C. Nason, T. J. Ruckwardt, J. S. McLellan, M. R. Denison, J. D. Chappell, I. N. Moore, K. M. Morabito, J. R. Mascola, R. S. Baric, A. Carfi, B. S. Graham, SARS-CoV-2 mRNA vaccine design enabled by prototype pathogen preparedness. *Nature* **586**, 567–571 (2020).
46. E. E. Walsh, R. W. Frenck Jr., A. R. Falsey, N. Kitchin, J. Absalon, A. Gurtman, S. Lockhart, K. Neuzil, M. J. Mulligan, R. Bailey, K. A. Swanson, P. Li, K. Koury, W. Kalina, D. Cooper, C. Fontes-Garfias, P.-Y. Shi, Ö. Türeci, K. R. Tompkins, K. E. Lyke, V. Raabe, P. R. Dormitzer, K. U. Jansen, U. Sahin, W. C. Gruber, Safety and immunogenicity of two RNA-based Covid-19 vaccine candidates. *N. Engl. J. Med.* **383**, 2439–2450 (2020).
47. J.-H. Tian, N. Patel, R. Haupt, H. Zhou, S. Weston, H. Hammond, J. Logue, A. D. Portnoff, J. Norton, M. Guebre-Xabier, B. Zhou, K. Jacobson, S. Maciejewski, R. Khatoun, M. Wisniewska, W. Moffitt, S. Kluepfel-Stahl, B. Ekechukwu, J. Papin, S. Boddapati, C. Jason Wong, P. A. Piedra, M. B. Frieman, M. J. Massare, L. Fries, K. L. Bengtsson, L. Stertman, L. Ellingsworth, G. Glenn, G. Smith, SARS-CoV-2 spike glycoprotein vaccine candidate NVX-CoV2373 immunogenicity in baboons and protection in mice. *Nat. Commun.* **12**, 372 (2021).
48. N. B. Mercado, R. Zahn, F. Wegmann, C. Loos, A. Chandrashekar, J. Yu, J. Liu, L. Peter, K. McMahan, L. H. Tostanoski, X. He, D. R. Martinez, L. Rutten, R. Bos, D. van Manen, J. Vellinga, J. Custers, J. P. Langedijk, T. Kwaks, M. J. G. Bakkers, D. Zuijdgheest, S. K. Rosendahl Huber, C. Atyeo, S. Fisinger, J. S. Burke, J. Feldman, B. M. Hauser, T. M. Caradonna, E. A. Bondzie, G. Dagotto, M. S. Gebre, E. Hoffman, C. Jacob-Dolan, M. Kirilova, Z. Li, Z. Lin, S. H. Mahrokhian, L. F. Maxfield, F. Nampanya, R. Nityanandam, J. P. Nkolola, S. Patel, J. D. Ventura, K. Verrington, H. Wan, L. Pessaint, A. Van Ry, K. Blade, A. Strasbaugh, M. Cabus, R. Brown, A. Cook, S. Zouantchangadou, E. Teow, H. Andersen, M. G. Lewis, Y. Cai, B. Chen, A. G. Schmidt, R. K. Reeves, R. S. Baric, D. A. Lauffenburger, G. Alter, P. Stoffels, M. Mammen, J. Van Hoof, H. Schuitemaker, D. H. Barouch, Single-shot Ad26 vaccine protects against SARS-CoV-2 in rhesus macaques. *Nature* **586**, 583–588 (2020).
49. P. M. Folegatti, K. J. Ewer, P. K. Aley, B. Angus, S. Becker, S. Belij-Rammerstorfer, D. Bellamy, S. Bibi, M. Bittaye, E. A. Clutterbuck, C. Dold, S. N. Faust, A. Finn, A. L. Flaxman, B. Hallis, P. Heath, D. Jenkin, R. Lazarus, R. Makinson, A. M. Minassian, K. M. Pollock, M. Ramasamy, H. Robinson, M. Snape, R. Tarrant, M. Voysey, C. Green, A. D. Douglas, A. V. S. Hill, T. Lambe, S. C. Gilbert, A. J. Pollard; Group, Oxford COVID Vaccine Trial, Safety and immunogenicity of the ChAdOx1 nCoV-19 vaccine against SARS-CoV-2: A preliminary report of a phase 1/2, single-blind, randomised controlled trial. *Lancet* **396**, 467–478 (2020).
50. D. Y. Logunov, I. V. Dolzhikova, O. V. Zubkova, A. I. Tukhvatulin, D. V. Shcheblyakov, A. S. Dzharullaeva, D. M. Grousova, A. S. Erokhova, A. V. Kovyrshina, A. G. Botikov, F. M. Ishaeva, O. Popova, T. A. Ozharovskaya, I. B. Esmagambetov, I. A. Favorskaya, D. I. Zrelkin, D. V. Voronina, D. N. Shcherbinina, A. S. Semikhin, Y. V. Simakova, E. A. Tokarskaya, N. L. Lubenets, D. A. Egorova, M. M. Shmarov, N. A. Nikitenko, L. F. Morozova, E. A. Smolyarchuk, E. V. Kryukov, V. F. Babira, S. V. Borisevich, B. S. Naroditsky, A. L. Gintsburg, Safety and immunogenicity of an rAd26 and rAd5 vector-based heterologous prime-boost COVID-19 vaccine in two formulations: Two open, non-randomised phase 1/2 studies from Russia. *Lancet* **396**, 887–897 (2020).
51. H. Wang, Y. Zhang, B. Huang, W. Deng, Y. Quan, W. Wang, W. Xu, Y. Zhao, N. Li, J. Zhang, H. Liang, L. Bao, Y. Xu, L. Ding, W. Zhou, H. Gao, J. Liu, P. Niu, L. Zhao, W. Zhen, H. Fu, S. Yu, Z. Zhang, G. Xu, C. Li, Z. Lou, M. Xu, C. Qin, G. Wu, G. F. Gao, W. Tan, X. Yang, Development of an inactivated vaccine candidate, BBIBP-CorV, with potent protection against SARS-CoV-2. *Cell* **182**, 713–721.e9 (2020).
52. T. Bedford, A. L. Greninger, P. Roychoudhury, L. M. Starita, M. Famulare, M.-L. Huang, A. Nalla, G. Pepper, A. Reinhardt, H. Xie, L. Shrestha, T. N. Nguyen, A. Adler, E. Brandstetter, S. Cho, D. Giroux, P. D. Han, K. Fay, C. D. Frazier, M. Ilcisin, K. Lacombe, J. Lee, A. Kiavand, M. Richardson, T. R. Sibley, M. Truong, C. R. Wolf, D. A. Nickerson, M. J. Rieder, J. A. England; Seattle Flu Study Investigators, J. Hadfield, E. B. Hodcroft, J. Huddleston, L. H. Moncla, N. F. Müller, R. A. Neher, X. Deng, W. Gu, S. Federman, C. Chiu, J. S. Duchin, R. Gautom, G. Melly, B. Hiatt, P. Dykema, S. Lindquist, K. Queen, Y. Tao, A. Uehara, S. Tong, D. MacCannell, G. L. Armstrong, G. S. Baird, H. Y. Chu, J. Shendure, K. R. Jerome, Cryptic transmission of SARS-CoV-2 in Washington state. *Science* **370**, 571–575 (2020).
53. J. E. Bowen, A. Addetia, H. V. Dang, C. Stewart, J. T. Brown, W. K. Sharkey, K. R. Sprouse, A. C. Walls, I. G. Mazzitelli, J. K. Logue, N. M. Franko, N. Czudnochowski, A. E. Powell, E. Dellota Jr., K. Ahmed, A. S. Ansari, E. Camerani, A. Gori, A. Bandera, C. M. Posavac, J. M. Dan, Z. Zhang, D. Weiskopf, A. Sette, S. Crotty, N. T. Iqbal, D. Corti, J. Geffner, G. Snell, R. Grifantini, H. Y. Chu, D. Veessler, Omicron spike function and neutralizing activity elicited by a comprehensive panel of vaccines. *Science* **377**, 890–894 (2022).
54. Z. Zhang, J. Mateus, C. H. Coelho, J. M. Dan, C. R. Moderbacher, R. I. Gálvez, F. H. Cortes, A. Grifoni, A. Tarke, J. Chang, E. A. Escarrega, C. Kim, B. Goodwin, N. I. Bloom, A. Frazier, D. Weiskopf, A. Sette, S. Crotty, Humoral and cellular immune memory to four COVID-19 vaccines. *Cell* **185**, 2434–2451.e17 (2022).
55. Z. Ke, J. Oton, K. Qu, M. Cortese, V. Zila, L. McKeane, T. Nakane, J. Zivanov, C. J. Neufeldt, B. Cerikan, J. M. Lu, J. Peukes, X. Xiong, H. G. Kräusslich, S. H. W. Scheres, R. Bartenschlager, J. A. G. Briggs, Structures and distributions of SARS-CoV-2 spike proteins on intact virions. *Nature* **588**, 498–502 (2020).
56. B. Turoňová, M. Sikora, C. Schürmann, W. J. H. Hagen, S. Welsch, F. E. C. Blanc, S. von Bülow, M. Gecht, K. Bagola, C. Hörner, G. van Zandbergen, J. Landry, N. T. D. de Azevedo, S. Mosalaganti, A. Schwarz, R. Covino, M. D. Mühlebach, G. Hummer, J. Krijnse Locker, M. Beck, In situ structural analysis of SARS-CoV-2 spike reveals flexibility mediated by three hinges. *Science* **370**, 203–208 (2020).
57. H. Yao, Y. Song, Y. Chen, N. Wu, J. Xu, C. Sun, J. Zhang, T. Weng, Z. Zhang, Z. Wu, L. Cheng, D. Shi, X. Lu, J. Lei, M. Crispin, Y. Shi, L. Li, S. Li, Molecular architecture of the SARS-CoV-2 virus. *Cell* **183**, 730–738.e13 (2020).
58. C. Liu, L. Mendonça, Y. Yang, Y. Gao, C. Shen, J. Liu, T. Ni, B. Ju, C. Liu, X. Tang, J. Wei, X. Ma, Y. Zhu, W. Liu, S. Xu, Y. Liu, J. Yuan, J. Wu, Z. Liu, Z. Zhang, L. Liu, P. Wang, P. Zhang, The architecture of inactivated SARS-CoV-2 with postfusion spikes revealed by cryo-EM and cryo-ET. *Structure* **28**, 1218–1224.e4 (2020).
59. L. Stamatatos, J. Czartoski, Y.-H. Wan, L. J. Homad, V. Rubin, H. Glantz, M. Meradilek, E. Seydoux, M. F. Jennewein, A. J. MacCamy, J. Feng, G. Mize, S. C. De Rosa, A. Finzi, M. P. Lemos, K. W. Cohen, Z. Moodie, M. J. McElrath, A. T. McGuire, mRNA vaccination boosts cross-variant neutralizing antibodies elicited by SARS-CoV-2 infection. *Science* **372**, 1413–1414 (2021).
60. F. Krammer, K. Srivastava, H. Alshammary, A. A. Amoako, M. H. Awawda, K. F. Beach, M. C. Bermúdez-González, D. A. Bielak, J. M. Carreño, R. L. Chernet, L. Q. Eaker, E. D. Ferreri, D. L. Floda, C. R. Gleason, J. Z. Hamburger, K. Jiang, G. Kleiner, D. Jurczyszak, J. C. Matthews, W. A. Mendez, I. Nabeel, L. C. F. Mulder, A. J. B. Ntusi, P. L. Russo, A.-B. T. Salimbangon, M. Saksena, A. S. Shin, G. Singh, L. A. Sominsky, D. Stadlbauer, A. Wajnberg, V. Simon, Antibody responses in seropositive persons after a single dose of SARS-CoV-2 mRNA vaccine. *N. Engl. J. Med.* **384**, 1372–1374 (2021).
61. R. Keeton, S. I. Richardson, T. Moyo-Gwete, T. Hermanus, M. B. Tincho, N. Benede, N. P. Manamela, R. Baguma, Z. Makhado, A. Ngomti, T. Motlou, M. Mennen, L. Chinhoyi, S. Skelem, H. Maboreke, D. Doolabh, A. Iranzadeh, A. D. Otter, T. Brooks, M. Noursadeghi, J. C. Moon, A. Grifoni, D. Weiskopf, A. Sette, J. Blackburn, N.-Y. Hsiao, C. Williamson, C. Riou, A. Goga, N. Garrett, L.-G. Bekker, G. Gray, N. A. B. Ntusi, P. L. Moore, W. A. Burgers, Prior infection with SARS-CoV-2 boosts and broadens Ad26.COV2.S immunogenicity in a variant-dependent manner. *Cell Host Microbe* **29**, 1611–1619.e5 (2021).
62. S. Saadat, Z. Rikhtegaran Tehrani, J. Logue, M. Newman, M. B. Frieman, A. D. Harris, M. M. Sajadi, Binding and neutralization antibody titers after a single vaccine dose in health care workers previously infected with SARS-CoV-2. *JAMA* **325**, 1467–1469 (2021).
63. A. C. Walls, X. Xiong, Y. J. Park, M. A. Tortorici, J. Snijder, J. Quispe, E. Camerani, R. Gopal, M. Dai, A. Lanzavecchia, M. Zamboni, F. A. Rey, D. Corti, D. Veessler, Unexpected receptor functional mimicry elucidates activation of coronavirus fusion. *Cell* **176**, 1026–1039.e15 (2019).
64. F. A. Lempp, L. Soriaga, M. Montiel-Ruiz, F. Benigni, J. Noack, Y.-J. Park, S. Bianchi, A. C. Walls, J. E. Bowen, J. Zhou, H. Kaiser, A. Joshi, M. Agostini, M. Meury, E. Dellota Jr., S. Jaconi, E. Camerani, J. Martinez-Picado, J. Vergara-Alert, N. Izquierdo-Useros, H. W. Virgin, A. Lanzavecchia, D. Veessler, L. Purcell, A. Telenti, D. Corti, Lectins enhance SARS-CoV-2 infection and influence neutralizing antibodies. *Nature* **598**, 342–347 (2021).
65. A. J. Greaney, A. N. Loes, L. E. Gentles, K. H. D. Crawford, T. N. Starr, K. D. Malone, H. Y. Chu, J. D. Bloom, Antibodies elicited by mRNA-1273 vaccination bind more broadly to the receptor binding domain than do those from SARS-CoV-2 infection. *Sci. Transl. Med.* **13**, eabi9915 (2021).
66. M. McCallum, J. Bassi, A. De Marco, A. Chen, A. C. Walls, J. Di Iulio, M. A. Tortorici, M.-J. Navarro, C. Silacci-Fregni, C. Saliba, K. R. Sprouse, M. Agostini, D. Pinto, K. Culp, S. Bianchi, S. Jaconi, E. Camerani, J. E. Bowen, S. W. Tilles, M. S. Pizzuto, S. B. Guastalla, G. Bona, A. F. Pellanda, C. Garzoni, W. C. Van Voorhis, L. E. Rosen, G. Snell, A. Telenti, H. W. Virgin, L. Piccoli, D. Corti, D. Veessler, SARS-CoV-2 immune evasion by the B.1.427/B.1.429 variant of concern. *Science* **373**, 648–654 (2021).
67. M. McCallum, A. C. Walls, K. R. Sprouse, J. E. Bowen, L. Rosen, H. V. Dang, A. De Marco, N. Franko, S. W. Tilles, J. Logue, M. C. Miranda, M. Ahlrichs, L. Carter, G. Snell, M. S. Pizzuto, H. Y. Chu, W. C. Van Voorhis, D. Corti, D. Veessler, Molecular basis of immune evasion by the delta and kappa SARS-CoV-2 variants. *Science* **374**, 1621–1626 (2021).
68. K. E. Kistler, J. Huddleston, T. Bedford, Rapid and parallel adaptive mutations in spike S1 drive clade success in SARS-CoV-2. *Cell Host Microbe* **30**, 545–555.e4 (2021).
69. M. Magro, V. Mas, K. Chappell, M. Vázquez, O. Cano, D. Luque, M. C. Terrón, J. A. Melero, C. Palomo, Neutralizing antibodies against the preactive form of respiratory syncytial virus

- fusion protein offer unique possibilities for clinical intervention. *Proc. Natl. Acad. Sci. U.S.A.* **109**, 3089–3094 (2012).
70. P. Sastre, J. A. Melero, B. Garcia-Barreno, C. Palomo, Comparison of affinity chromatography and adsorption to vaccinia virus recombinant infected cells for depletion of antibodies directed against respiratory syncytial virus glycoproteins present in a human immunoglobulin preparation. *J. Med. Virol.* **76**, 248–255 (2005).
  71. W. Dejnirattisai, D. Zhou, H. M. Ginn, H. M. E. Duyvesteyn, P. Supasa, J. B. Case, Y. Zhao, T. S. Walter, A. J. Mentzer, C. Liu, B. Wang, G. C. Paesen, J. Slon-Campos, C. López-Camacho, N. M. Kafai, A. L. Bailey, R. E. Chen, B. Ying, C. Thompson, J. Bolton, A. Fyfe, S. Gupta, T. K. Tan, J. Gilbert-Jaramillo, W. James, M. Knight, M. W. Carroll, D. Skelly, C. Dold, Y. Peng, R. Levin, T. Dong, A. J. Pollard, T. C. Knight, P. Klenerman, N. Temperton, D. R. Hall, M. A. Williams, N. G. Paterson, F. K. R. Bertram, C. A. Seibert, D. K. Clare, A. Howe, J. Raedecke, Y. Song, A. R. Townsend, K.-Y. A. Huang, E. E. Fry, J. Mongkolsapaya, M. S. Diamond, J. Ren, D. I. Stuart, G. R. Screaton, The antigenic anatomy of SARS-CoV-2 receptor binding domain. *Cell* **184**, 2183–2200.e22 (2021).
  72. K. H. D. Crawford, R. Eguia, A. S. Dingens, A. N. Loes, K. D. Malone, C. R. Wolf, H. Y. Chu, M. A. Tortorici, D. Velesler, M. Murphy, D. Pettie, N. P. King, A. B. Balazs, J. D. Bloom, Protocol and reagents for pseudotyping lentiviral particles with SARS-CoV-2 spike protein for neutralization assays. *Viruses* **12**, 513 (2020).
  73. D. A. Collier, A. De Marco, I. A. T. M. Ferreira, B. Meng, R. Datir, A. C. Walls, S. A. Kemp, J. Bassi, D. Pinto, C. S. Fregni, S. Bianchi, M. A. Tortorici, J. Bowen, K. Culap, S. Jaconi, E. Cameroni, G. Snell, M. S. Pizzuto, A. F. Pellanda, C. Garzoni, A. Riva, A. Elmer, N. Kingston, B. Graves, L. E. McCoy, K. G. C. Smith, J. R. Bradley, N. Temperton, L. Lourdes Ceron-Gutierrez, G. Barcenas-Morales, W. Harvey, H. W. Virgin, A. Lanzavecchia, L. Piccoli, R. Doffinger, M. Wills, D. Velesler, D. Corti, R. K. Gupta; The CITIID-NIHR BioResource COVID-19 Collaboration; The COVID-19 Genomics UK (COG-UK) consortium, Sensitivity of SARS-CoV-2 B.1.1.7 to mRNA vaccine-elicited antibodies. *Nature* **593**, 136–141 (2021).
  74. D. Weissman, M.-G. Alameh, T. de Silva, P. Collini, H. Hornsby, R. Brown, C. C. LaBranche, R. J. Edwards, L. Sutherland, S. Santra, K. Mansouri, S. Gobeil, C. McDanal, N. Pardi, N. Hengartner, P. J. C. Lin, Y. Tam, P. A. Shaw, M. G. Lewis, C. Boesler, U. Şahin, P. Acharya, B. F. Haynes, B. Korber, D. C. Montefiori, D614G spike mutation increases SARS CoV-2 susceptibility to neutralization. *Cell Host Microbe* **29**, 23–31.e4 (2021).
  75. P. Mlcochova, S. Kemp, M. S. Dhar, G. Papa, B. Meng, I. A. T. M. Ferreira, R. Datir, D. A. Collier, A. Albecka, S. Singh, R. Pandey, J. Brown, J. Zhou, N. Goonawardane, S. Mishra, C. Whittaker, T. Mellan, R. Marwal, M. Datta, S. Sengupta, K. Ponnusamy, V. S. Radhakrishnan, A. Abdullahi, O. Charles, P. Chattopadhyay, P. Devi, D. Caputo, T. Peacock, D. C. Wattal, N. Goel, A. Satwik, R. Vaishya, M. Agarwal; Indian SARS-CoV-2 Genomics Consortium (INSACOG); Genotype to Phenotype Japan (G2P-Japan) Consortium; CITIID-NIHR BioResource COVID-19 Collaboration, A. Mavousian, J. H. Lee, J. Bassi, C. Silacci-Fegni, C. Saliba, D. Pinto, T. Irie, I. Yoshida, W. L. Hamilton, K. Sato, S. Bhatt, S. Flaxman, L. C. James, D. Corti, L. Piccoli, W. S. Barclay, P. Rakshit, A. Agrawal, R. K. Gupta, SARS-CoV-2 B.1.617.2 Delta variant replication and immune evasion. *Nature* **599**, 114–119 (2021).
  76. Y.-J. Park, A. De Marco, T. N. Starr, Z. Liu, D. Pinto, A. C. Walls, F. Zatta, S. K. Zepeda, J. Bowen, K. S. Sprouse, A. Joshi, M. Giurdanella, B. Guarino, J. Noack, R. Abdelnabi, S.-Y. C. Foo, F. A. Lempp, F. Benigni, G. Snell, J. Neyts, S. P. J. Whelan, H. W. Virgin, J. D. Bloom, D. Corti, M. S. Pizzuto, D. Velesler, Antibody-mediated broad sarbecovirus neutralization through ACE2 molecular mimicry. *Science* **375**, 449–454 (2022).
  77. A. Z. Wee, D. Wrapp, A. S. Herbert, D. P. Maurer, D. Haslwanter, M. Sakharkar, R. K. Jangra, M. E. Dieterle, A. Lilov, D. Huang, L. V. Tse, N. V. Johnson, C. L. Hsieh, N. Wang, J. H. Nett, E. Champney, I. Burnina, M. Brown, S. Lin, M. Sinclair, C. Johnson, S. Pudi, R. Bortz, A. S. Wirchanski, E. Laudermitch, C. Florez, J. M. Fels, C. M. O'Brien, B. S. Graham, D. Nemazee, D. R. Burton, R. S. Baric, J. E. Voss, K. Chandran, J. M. Dye, J. S. McLellan, L. M. Walker, Broad neutralization of SARS-related viruses by human monoclonal antibodies. *Science* **369**, 731–736 (2020).
  78. C. G. Rappazzo, L. V. Tse, C. I. Kaku, D. Wrapp, M. Sakharkar, D. Huang, L. M. Deveau, T. J. Yockachonis, A. S. Herbert, M. B. Battles, C. M. O'Brien, M. E. Brown, J. C. Geoghegan, J. Belk, L. Peng, L. Yang, Y. Hou, T. D. Scobey, D. R. Burton, D. Nemazee, J. M. Dye, J. E. Voss, B. M. Gunn, J. S. McLellan, R. S. Baric, L. E. Gralinski, L. M. Walker, Broad and potent activity against SARS-like viruses by an engineered human monoclonal antibody. *Science* **371**, 823–829 (2021).
  79. Y.-J. Park, D. Pinto, A. C. Walls, Z. Liu, A. De Marco, F. Benigni, F. Zatta, C. Silacci-Fegni, J. Bassi, K. R. Sprouse, A. Addetia, J. E. Bowen, C. Stewart, M. Giurdanella, C. Saliba, B. Guarino, M. A. Schmid, N. Franko, J. Logue, H. V. Dang, K. Hauser, J. di Iulio, W. Rivera, G. Schnell, F. A. Lempp, J. Janer, R. Abdelnabi, P. Maes, P. Ferrari, A. Ceschi, O. Giannini, G. D. de Melo, L. Kergoat, H. Bourhy, J. Neyts, L. Soriaga, L. A. Purcell, G. Snell, S. P. J. Whelan, A. Lanzavecchia, H. W. Virgin, L. Piccoli, H. Chu, M. S. Pizzuto, D. Corti, D. Velesler, Imprinted antibody responses against SARS-CoV-2 Omicron sublineages. *Science*, eadc9127 (2022).
  80. K. Westendorf, S. Žentelis, L. Wang, D. Foster, P. Vaillancourt, M. Wiggin, E. Lovett, R. van der Lee, J. Hendle, A. Pustilnik, J. M. Sauder, L. Kraft, Y. Hwang, R. W. Siegel, J. Chen, B. A. Heinz, R. E. Higgs, N. L. Kallewaard, K. Jepson, R. Goya, M. A. Smith, D. W. Collins, D. Pellacani, P. Xiang, V. de Puyraimond, M. Ricicova, L. Devorkin, C. Pritchard, A. O'Neill, K. Dalal, P. Panwar, H. Dhupar, F. A. Garces, C. A. Cohen, J. M. Dye, K. E. Huie, C. V. Badger, D. Kobasa, J. A. Audet, J. J. Freitas, S. Hassanali, I. Hughes, L. Munoz, H. C. Palma, B. Ramamurthy, R. W. Cross, T. W. Geisbert, V. Menachery, K. Lokugamage, V. Borisevich, I. Lanz, L. Anderson, P. Sipahimalani, K. S. Corbett, E. S. Yang, Y. Zhang, W. Shi, T. Zhou, M. Choe, J. Misasi, P. D. Kwong, N. J. Sullivan, B. S. Graham, T. L. Fernandez, C. L. Hansen, E. Falconer, J. R. Mascola, B. E. Jones, B. C. Barnhart, LY-CoV1404 (bebtelovimab) potently neutralizes SARS-CoV-2 variants. *Cell Rep.* **39**, 110812 (2022).
  81. D. R. Martinez, A. Schäfer, S. Gobeil, D. Li, G. De la Cruz, R. Parks, X. Lu, M. Barr, V. Stalls, K. Janowska, E. Beaudoin, K. Manne, K. Mansouri, R. J. Edwards, K. Cronin, B. Yount, K. Anasti, S. A. Montgomery, J. Tang, H. Golding, S. Shen, T. Zhou, P. D. Kwong, B. S. Graham, J. R. Mascola, D. C. Montefiori, S. M. Alam, G. D. Sempowski, S. Khurana, K. Wiehe, K. O. Saunders, P. Acharya, B. F. Haynes, R. S. Baric, A broadly cross-reactive antibody neutralizes and protects against sarbecovirus challenge in mice. *Sci. Transl. Med.* **14**, eabj7125 (2021).
  82. C. A. Jette, A. A. Cohen, P. N. P. Gnanaprasgam, F. Muecksch, Y. E. Lee, K. E. Huey-Tubman, F. Schmidt, T. Hatziioannou, P. D. Bieniasz, M. C. Nussenzweig, A. P. West Jr., J. R. Keeffe, P. J. Bjorkman, C. O. Barnes, Broad cross-reactivity across sarbecoviruses exhibited by a subset of COVID-19 donor-derived neutralizing antibodies. *Cell Rep.* **36**, 109760 (2021).
  83. E. Cameroni, J. E. Bowen, L. E. Rosen, C. Saliba, S. K. Zepeda, K. Culap, D. Pinto, L. A. VanBlargan, A. De Marco, J. di Iulio, F. Zatta, H. Kaiser, J. Noack, N. Farhat, N. Czudnochowski, K. Havenar-Daughton, K. R. Sprouse, J. R. Dillen, A. E. Powell, A. Chen, C. Maher, L. Yin, D. Sun, L. Soriaga, J. Bassi, C. Silacci-Fegni, C. Gustafsson, N. M. Franko, J. Logue, N. T. Iqbal, I. Mazzitelli, J. Geffner, R. Grifantini, H. Chu, A. Gori, A. Riva, O. Giannini, A. Ceschi, P. Ferrari, P. E. Cippà, A. Franzetti-Pellanda, C. Garzoni, P. J. Halfmann, Y. Kawaoka, C. Hebnner, L. A. Purcell, L. Piccoli, M. S. Pizzuto, A. C. Walls, M. S. Diamond, A. Telenti, H. W. Virgin, A. Lanzavecchia, G. Snell, D. Velesler, D. Corti, Broadly neutralizing antibodies overcome SARS-CoV-2 Omicron antigenic shift. *Nature* **602**, 664–670 (2021).
  84. L. Liu, S. Iketani, Y. Guo, J. F.-W. Chan, M. Wang, L. Liu, Y. Luo, H. Chu, Y. Huang, M. S. Nair, J. Yu, K. K.-H. Chik, T. T.-T. Yuen, C. Yoon, K. K.-W. To, H. Chen, M. T. Yin, M. E. Sobieszczyk, Y. Huang, H. H. Wang, Z. Sheng, K.-Y. Yuen, D. D. Ho, Striking antibody evasion manifested by the Omicron variant of SARS-CoV-2. *Nature* **602**, 676–681 (2021).
  85. J. S. McLellan, M. Chen, M. G. Joyce, M. B. Stewart-Jones, Y. Yang, B. Zhang, L. Chen, S. Srivatsan, A. Zheng, T. Zhou, K. W. Graepel, A. Kumar, S. Moin, J. C. Boyington, G. Y. Chuang, C. Soto, U. Baxa, A. Q. Bakker, H. Spits, T. Beaumont, Z. Zheng, N. Xia, S. Y. Ko, J. P. Todd, S. Rao, B. S. Graham, P. D. Kwong, Structure-based design of a fusion glycoprotein vaccine for respiratory syncytial virus. *Science* **342**, 592–598 (2013).
  86. J. S. McLellan, M. Chen, S. Leung, K. W. Graepel, X. Du, Y. Yang, T. Zhou, U. Baxa, E. Yasuda, T. Beaumont, A. Kumar, K. Modjarrad, Z. Zheng, M. Zhao, N. Xia, P. D. Kwong, B. S. Graham, Structure of RSV fusion glycoprotein trimer bound to a prefusion-specific neutralizing antibody. *Science* **340**, 1113–1117 (2013).
  87. T. J. Ruckwardt, K. M. Morabito, E. Phung, M. C. Crank, P. J. Costner, L. A. Holman, L. A. Chang, S. P. Hickman, N. M. Berkowitz, I. J. Gordon, G. V. Yamshchikov, M. R. Gaudinski, B. Lin, R. Bailor, M. Chen, A. M. Ortega-Villa, T. Nguyen, A. Kumar, R. M. Schwartz, L. A. Kuelzto, J. A. Stein, K. Carlton, J. G. Gall, M. C. Nason, J. R. Mascola, G. Chen, B. S. Graham, A. Arthur, J. Cunningham, A. Eshun, B. Larkin, F. Mendoza, L. Novik, J. Saunders, X. Wang, W. Whalen, C. Carter, C. S. Hendel, S. Plummer, A. Ola, A. Widge, M. C. Burgos Florez, L. Le, I. Pittman, R. S. S. Rothwell, O. Trofyomenko, O. Vasilenko, P. Apte, R. Hicks, C. T. Cartagena, P. Williams, L. Requilman, C. Tran, S. Bai, E. Carey, A. L. Chamberlain, Y.-C. Chang, M. Chen, P. Chen, J. Cooper, C. Fridley, M. Ghosh, D. Gollapudi, J. Holland-Linn, J. Horwitz, A. Hussain, V. Ivleva, F. Kaltovich, K. Leach, C. Lee, A. Liu, X. Liu, S. Manceva, A. Menon, A. Nagy, S. O'Connell, R. Raguathan, J. Walters, Z. Zhao, Safety, tolerability, and immunogenicity of the respiratory syncytial virus pre-fusion F subunit vaccine DS-Cav1: A phase 1, randomised, open-label, dose-escalation clinical trial. *Lancet Respir. Med.* **9**, 1111–1120 (2021).
  88. B. Schmoele-Thoma, A. M. Zareba, Q. Jiang, M. S. Maddur, R. Danaf, A. Mann, K. Eze, J. Fok-Seang, G. Kabir, A. Catchpole, D. A. Scott, A. C. Gurtman, K. U. Jansen, W. C. Gruber, P. R. Dormitzer, K. A. Swanson, Vaccine efficacy in adults in a respiratory syncytial virus challenge study. *N. Engl. J. Med.* **386**, 2377–2386 (2022).
  89. C. Dacon, C. Tucker, L. Peng, C.-C. D. Lee, T.-H. Lin, M. Yuan, Y. Cong, L. Wang, L. Purser, J. K. Williams, C.-W. Pyo, I. Kosik, Z. Hu, M. Zhao, D. Mohan, A. J. R. Cooper, M. Peterson, J. Skinner, S. Dixit, E. Kollins, L. Huzella, D. Perry, R. Byrum, S. Lembirik, D. Drawbaugh, B. Eaton, Y. Zhang, E. S. Yang, M. Chen, K. Leung, R. S. Weinberg, A. Pegu, D. E. Geraghty, E. Davidson, I. Douagi, S. Moir, J. W. Yewdell, C. Schmaljohn, P. D. Crompton, M. R. Holbrook, D. Nemazee, J. R. Mascola, I. A. Wilson, J. Tan, Broadly neutralizing antibodies target the coronavirus fusion peptide. *Science* **377**, 728–735 (2022).
  90. F. Amanat, S. Strohmeier, R. Rathnasinghe, M. Schotsaert, L. Coughlan, A. García-Sastre, F. Krammer, Introduction of two prolines and removal of the polybasic cleavage site lead

- to higher efficacy of a recombinant spike-based SARS-CoV-2 vaccine in the mouse model. *MBio* **12**, e02648-20 (2021).
91. C. L. Hsieh, J. A. Goldsmith, J. M. Schaub, A. M. DiVenere, H. C. Kuo, K. Javanmardi, K. C. Le, D. Wrapp, A. G. Lee, Y. Liu, C. W. Chou, P. O. Byrne, C. K. Hjorth, N. V. Johnson, J. Ludes-Meyers, A. W. Nguyen, J. Park, N. Wang, D. Amengor, J. J. Lavinder, G. C. Ippolito, J. A. Maynard, I. J. Finkelstein, J. S. McLellan, Structure-based design of prefusion-stabilized SARS-CoV-2 spikes. *Science* **369**, 1501–1505 (2020).
  92. E. Olmedillas, C. J. Mann, W. Peng, Y. T. Wang, R. D. Avalos, Structure-based design of a highly stable, covalently-linked SARS-CoV-2 spike trimer with improved structural properties and immunogenicity. *bioRxiv* 2021.05.06.4410465 (2021). [www.biorxiv.org/content/10.1101/2021.05.06.441046v1.abstract](http://www.biorxiv.org/content/10.1101/2021.05.06.441046v1.abstract).
  93. D. R. Martinez, A. Schaefer, S. Gobeil, D. Li, G. De la Cruz, R. Parks, X. Lu, M. Barr, K. Manne, K. Mansouri, R. J. Edwards, B. Yount, K. Anasti, S. A. Montgomery, S. Shen, T. Zhou, P. D. Kwong, B. S. Graham, J. R. Mascola, D. C. Montefiori, M. Alam, G. D. Sempowski, K. Wiehe, K. O. Saunders, P. Acharya, B. F. Haynes, R. S. Baric, A broadly neutralizing antibody protects against SARS-CoV, pre-emergent bat CoVs, and SARS-CoV-2 variants in mice. *bioRxiv* 2021.04.27.441655 (2021). <https://doi.org/10.1101/2021.04.27.441655>.
  94. E. S. Winkler, P. Gilchuk, J. Yu, A. L. Bailey, R. E. Chen, Z. Chong, S. J. Zost, H. Jang, Y. Huang, J. D. Allen, J. B. Case, R. E. Sutton, R. H. Carnahan, T. L. Darling, A. C. M. Boon, M. Mack, R. D. Head, T. M. Ross, J. E. Crowe Jr., M. S. Diamond, Human neutralizing antibodies against SARS-CoV-2 require intact Fc effector functions for optimal therapeutic protection. *Cell* **184**, 1804–1820.e16 (2021).
  95. A. Schäfer, F. Muecksch, J. C. C. Lorenzi, S. R. Leist, M. Cipolla, S. Bournazos, F. Schmidt, R. M. Maisson, A. Gazumyan, D. R. Martinez, R. S. Baric, D. F. Robbiani, T. Hatziioannou, J. V. Ravetch, P. D. Bieniasz, R. A. Bowen, M. C. Nussenzweig, T. P. Sheahan, Antibody potency, effector function, and combinations in protection and therapy for SARS-CoV-2 infection in vivo. *J. Exp. Med.* **218**, e20201993 (2021).
  96. J. B. Case, S. Mackin, J. M. Errico, Z. Chong, E. A. Madden, B. Whitener, B. Guarino, M. A. Schmid, K. Rosenthal, K. Ren, H. V. Dang, G. Snell, A. Jung, L. Droit, S. A. Handley, P. J. Halfmann, Y. Kawaoka, J. E. Crowe Jr., D. H. Fremont, H. W. Virgin, Y.-M. Loo, M. T. Esser, L. A. Purcell, D. Corti, M. S. Diamond, Resilience of S309 and AZD7442 monoclonal antibody treatments against infection by SARS-CoV-2 Omicron lineage strains. *Nat. Commun.* **13**, 3824 (2022).
  97. D. Y. Zhu, M. J. Gorman, D. Yuan, J. Yu, N. B. Mercado, K. McMahan, E. N. Borducchi, M. Lifton, J. Liu, F. Nampanya, S. Patel, L. H. Tostanoski, L. Pessaint, A. Van Ry, B. Finneyfrock, J. Velasco, E. Teow, R. Brown, A. Cook, H. Andersen, M. G. Lewis, D. A. Lauffenburger, D. H. Barouch, G. Alter, Defining the determinants of protection against SARS-CoV-2 infection and viral control in a dose-down Ad26.CoV2.S vaccine study in nonhuman primates. *PLOS Biol.* **20**, e3001609 (2022).
  98. Y. C. Bartsch, X. Tong, J. Kang, M. J. Avedaño, E. F. Serrano, T. García-Salum, C. Pardo-Roa, A. Riquelme, Y. Cai, I. Renzi, G. Stewart-Jones, B. Chen, R. A. Medina, G. Alter, Omicron variant Spike-specific antibody binding and Fc activity are preserved in recipients of mRNA or inactivated COVID-19 vaccines. *Sci. Transl. Med.* **14**, eabn9243 (2022).
  99. P. Kaplonek, S. Fischinger, D. Cizmeki, Y. C. Bartsch, J. Kang, J. S. Burke, S. A. Shin, D. Dayal, P. Martin, C. Mann, F. Amanat, B. Julg, E. J. Nilles, E. R. Musk, A. S. Menon, F. Krammer, E. O. Saphire, A. Carfi, G. Alter, mRNA-1273 vaccine-induced antibodies maintain Fc effector functions across SARS-CoV-2 variants of concern. *Immunity* **55**, 355–365.e4 (2022).
  100. A. C. Walls, B. Fiala, A. Schäfer, S. Wrenn, M. N. Pham, M. Murphy, L. V. Tse, L. Shehata, M. A. O'Connor, C. Chen, M. J. Navarro, M. C. Miranda, D. Pettie, R. Ravichandran, J. C. Kraft, C. Ogohara, A. Palser, S. Chalk, E. C. Lee, K. Guerriero, E. Kepl, C. M. Chow, C. Sydeman, E. A. Hodge, B. Brown, J. T. Fuller, K. H. Dinno, L. E. Gralinski, S. R. Leist, K. L. Gully, T. B. Lewis, M. Guttman, H. Y. Chu, K. K. Lee, D. H. Fuller, R. S. Baric, P. Kellam, L. Carter, M. Pepper, T. P. Sheahan, D. Veelsler, N. P. King, Elicitation of potent neutralizing antibody responses by designed protein nanoparticle vaccines for SARS-CoV-2. *Cell* **183**, 1367–1382.e17 (2020).
  101. K. O. Saunders, E. Lee, R. Parks, D. R. Martinez, D. Li, H. Chen, R. J. Edwards, S. Gobeil, M. Barr, K. Mansouri, S. M. Alam, L. L. Sutherland, F. Cai, A. M. Sanzone, M. Berry, K. Manne, K. W. Bock, M. Minai, B. M. Nagata, A. B. Kapingidza, M. Azoitei, L. V. Tse, T. D. Scobey, R. L. Spreng, R. W. Rountree, C. T. DeMarco, T. N. Denny, C. W. Woods, E. W. Petzold, J. Tang, T. H. Oguin 3rd, G. D. Sempowski, M. Gagne, D. C. Douek, M. A. Tomai, C. B. Fox, R. Seder, K. Wiehe, D. Weissman, N. Pardi, H. Golding, S. Khurana, P. Acharya, H. Andersen, M. G. Lewis, I. N. Moore, D. C. Montefiori, R. S. Baric, B. F. Haynes, Neutralizing antibody vaccine for pandemic and pre-emergent coronaviruses. *Nature* **594**, 553–559 (2021).
  102. H. A. D. King, M. G. Joyce, I. Lakhall-Naouar, A. Ahmed, C. M. Cincotta, C. Subra, K. K. Peachman, H. R. Hack, R. E. Chen, P. V. Thomas, W.-H. Chen, R. S. Sankhala, A. Hajduczki, E. J. Martinez, C. E. Peterson, W. C. Chang, M. Choe, C. Smith, J. A. Headley, H. A. Elyard, A. Cook, A. Anderson, K. M. Wuertz, M. Dong, I. Swafford, J. B. Case, J. R. Currier, K. G. Lal, M. F. Amare, V. Dussupt, S. Molnar, S. P. Daye, X. Zeng, E. K. Barkei, K. Alfson, H. M. Staples, R. Carrion, S. J. Krebs, D. Paquin-Proulx, N. Karasavvas, V. R. Polonis, L. L. Jagodzinski, S. Vasan, P. T. Scott, Y. Huang, M. S. Nair, D. D. Ho, N. de Val, M. S. Diamond, M. G. Lewis, M. Rao, G. R. Matyas, G. D. Gromowski, S. A. Peel, N. L. Michael, K. Modjarrad, D. L. Bolton, Efficacy and breadth of adjuvanted SARS-CoV-2 receptor-binding domain nanoparticle vaccine in macaques. *Proc. Natl. Acad. Sci. U.S.A.* **118**, e2106433118 (2021).
  103. K. M. Wuertz, E. K. Barkei, W.-H. Chen, E. J. Martinez, I. Lakhall-Naouar, L. L. Jagodzinski, D. Paquin-Proulx, G. D. Gromowski, I. Swafford, A. Ganesh, M. Dong, X. Zeng, P. V. Thomas, R. S. Sankhala, A. Hajduczki, C. E. Peterson, C. Kuklis, S. Soman, L. Wiczorek, M. Zemil, A. Anderson, J. Darden, H. Hernandez, H. Grove, V. Dussupt, H. Hack, R. de la Barrera, S. Zarling, J. F. Wood, J. W. Froude, M. Gagne, A. R. Henry, E. B. Mokhtari, P. Mudvari, S. J. Krebs, A. S. Pekosz, J. R. Currier, S. Kar, M. Porto, A. Winn, K. Radzyminski, M. G. Lewis, S. Vasan, M. Suthar, V. R. Polonis, G. R. Matyas, E. A. Boritz, D. C. Douek, R. A. Seder, S. P. Daye, M. Rao, S. A. Peel, M. G. Joyce, D. L. Bolton, N. L. Michael, K. Modjarrad, A SARS-CoV-2 spike ferritin nanoparticle vaccine protects hamsters against Alpha and Beta virus variant challenge. *NPJ Vaccines*. **6**, 129 (2021).
  104. J. Y. Song, W. S. Choi, J. Y. Heo, J. S. Lee, D. S. Jung, S.-W. Kim, K.-H. Park, J. S. Eom, S. J. Jeong, J. Lee, K. T. Kwon, H. J. Choi, J. W. Sohn, Y. K. Kim, J. Y. Noh, W. J. Kim, F. Roman, M. A. Ceregado, F. Solmi, A. Philpott, A. C. Walls, L. Carter, D. Veelsler, N. P. King, H. Kim, J. H. Ryu, S. J. Lee, Y. W. Park, H. K. Park, H. J. Cheong, Safety and immunogenicity of a SARS-CoV-2 recombinant protein nanoparticle vaccine (GBP510) adjuvanted with AS03: A randomised, placebo-controlled, observer-blinded phase 1/2 trial. *EClinicalMedicine* **51**, 101569 (2022).
  105. A. C. Walls, M. C. Miranda, A. Schäfer, M. N. Pham, A. Greaney, P. S. Arunachalam, M.-J. Navarro, M. A. Tortorici, K. Rogers, M. A. O'Connor, L. Shirreff, D. E. Ferrell, J. Bowen, N. Brunette, E. Kepl, S. K. Zepeda, T. Starr, C.-L. Hsieh, B. Fiala, S. Wrenn, D. Pettie, C. Sydeman, K. R. Sprouse, M. Johnson, A. Blackstone, R. Ravichandran, C. Ogohara, L. Carter, S. W. Tilles, R. Rappuoli, S. R. Leist, D. R. Martinez, M. Clark, R. Tisch, D. T. O'Hagan, R. Van Der Most, W. C. Van Voorhis, D. Corti, J. S. McLellan, H. Klebanoff, T. P. Sheahan, K. D. Smith, D. H. Fuller, F. Villinger, J. Bloom, B. Pulendran, R. Baric, N. P. King, D. Veelsler, Elicitation of broadly protective sarbecovirus immunity by receptor-binding domain nanoparticle vaccines. *Cell* **184**, 5432–5447.e16 (2021).
  106. A. A. Cohen, P. N. P. Gnanapragasam, Y. E. Lee, P. R. Hoffman, S. Ou, L. M. Kakutani, J. R. Keeffe, H.-J. Wu, M. Howarth, A. P. West, C. O. Barnes, M. C. Nussenzweig, P. J. Bjorkman, Mosaic nanoparticles elicit cross-reactive immune responses to zoonotic coronaviruses in mice. *Science* **371**, 735–741 (2021).
  107. A. A. Cohen, N. van Doremalen, A. J. Greaney, H. Andersen, A. Sharma, T. N. Starr, J. R. Keeffe, C. Fan, J. E. Schulz, P. N. P. Gnanapragasam, L. M. Kakutani, A. P. West Jr., G. Saturday, Y. E. Lee, H. Gao, C. A. Jette, M. G. Lewis, T. K. Tan, A. R. Townsend, J. D. Bloom, V. J. Munster, P. J. Bjorkman, Mosaic RBD nanoparticles protect against challenge by diverse sarbecoviruses in animal models. *Science* **377**, eabq0839 (2022).
  108. D. R. Martinez, A. Schäfer, S. R. Leist, G. De la Cruz, A. West, E. N. Atochina-Vasserman, L. C. Lindesmith, N. Pardi, R. Parks, M. Barr, D. Li, B. Yount, K. O. Saunders, D. Weissman, B. F. Haynes, S. A. Montgomery, R. S. Baric, Chimeric spike mRNA vaccines protect against Sarbecovirus challenge in mice. *Science* **373**, 991–998 (2021).
  109. J. B. Case, P. W. Rothlauf, R. E. Chen, Z. Liu, H. Zhao, A. S. Kim, L. M. Bloyet, Q. Zeng, S. Tahan, L. Droit, M. X. G. Ilagan, M. A. Tartell, G. Amarasinghe, J. P. Henderson, S. Miersch, M. Ustav, S. Sidhu, H. W. Virgin, D. Wang, S. Ding, D. Corti, E. S. Theel, D. H. Fremont, M. S. Diamond, S. P. J. Whelan, Neutralizing antibody and soluble ACE2 inhibition of a replication-competent VSV-SARS-CoV-2 and a clinical isolate of SARS-CoV-2. *Cell Host Microbe* **28**, 475–485.e5 (2020).
  110. X. Ou, Y. Liu, X. Lei, P. Li, D. Mi, L. Ren, L. Guo, R. Guo, T. Chen, J. Hu, Z. Xiang, Z. Mu, X. Chen, J. Chen, K. Hu, Q. Jin, J. Wang, Z. Qian, Characterization of spike glycoprotein of SARS-CoV-2 on virus entry and its immune cross-reactivity with SARS-CoV. *Nat. Commun.* **11**, 1620 (2020).
  111. C. J. Russo, L. A. Passmore, Electron microscopy: Ultrastable gold substrates for electron cryomicroscopy. *Science* **346**, 1377–1380 (2014).
  112. C. Suloway, J. Pulokas, D. Fellmann, A. Cheng, F. Guerra, J. Quispe, S. Stagg, C. S. Potter, B. Carragher, Automated molecular microscopy: The new Legion system. *J. Struct. Biol.* **151**, 41–60 (2005).
  113. D. Tegunov, P. Cramer, Real-time cryo-electron microscopy data preprocessing with Warp. *Nat. Methods* **16**, 1146–1152 (2019).
  114. A. Punjani, J. L. Rubinstein, D. J. Fleet, M. A. Brubaker, cryoSPARC: Algorithms for rapid unsupervised cryo-EM structure determination. *Nat. Methods* **14**, 290–296 (2017).
  115. J. Zivanov, T. Nakane, B. O. Forsberg, D. Kimanius, W. J. Hagen, E. Lindahl, S. H. Scheres, New tools for automated high-resolution cryo-EM structure determination in RELION-3. *eLife* **7**, e42166 (2018).
  116. A. Punjani, H. Zhang, D. J. Fleet, Non-uniform refinement: Adaptive regularization improves single-particle cryo-EM reconstruction. *Nat. Methods* **17**, 1214–1221 (2020).
  117. J. Zivanov, T. Nakane, S. H. W. Scheres, A Bayesian approach to beam-induced motion correction in cryo-EM single-particle analysis. *IUCr*. **6**, 5–17 (2019).

118. P. B. Rosenthal, R. Henderson, Optimal determination of particle orientation, absolute hand, and contrast loss in single-particle electron cryomicroscopy. *J. Mol. Biol.* **333**, 721–745 (2003).
119. S. Chen, G. McMullan, A. R. Faruqi, G. N. Murshudov, J. M. Short, S. H. Scheres, R. Henderson, High-resolution noise substitution to measure overfitting and validate resolution in 3D structure determination by single particle electron cryomicroscopy. *Ultramicroscopy* **135**, 24–35 (2013).
120. E. F. Pettersen, T. D. Goddard, C. C. Huang, G. S. Couch, D. M. Greenblatt, E. C. Meng, T. E. Ferrin, UCSF Chimera—A visualization system for exploratory research and analysis. *J. Comput. Chem.* **25**, 1605–1612 (2004).
121. P. Emsley, B. Lohkamp, W. G. Scott, K. Cowtan, Features and development of Coot. *Acta Crystallogr. D Biol. Crystallogr.* **66**, 486–501 (2010).
122. B. Frenz, S. Rämisch, A. J. Borst, A. C. Walls, J. Adolf-Bryfogle, W. R. Schief, D. Veeler, F. DiMaio, Automatically fixing errors in glycoprotein structures with Rosetta. *Structure* **27**, 134–139.e3 (2019).
123. R. Y. Wang, Y. Song, B. A. Barad, Y. Cheng, J. S. Fraser, F. DiMaio, Automated structure refinement of macromolecular assemblies from cryo-EM maps using Rosetta. *eLife* **5**, e17219 (2016).
124. V. B. Chen, W. B. Arendall, J. J. Headd, D. A. Keedy, R. M. Immormino, G. J. Kapral, L. W. Murray, J. S. Richardson, D. C. Richardson, MolProbity: All-atom structure validation for macromolecular crystallography. *Acta Crystallogr. D Biol. Crystallogr.* **66**, 12–21 (2010).
125. B. A. Barad, N. Echols, R. Y. Wang, Y. Cheng, F. DiMaio, P. D. Adams, J. S. Fraser, EMRinger: Side chain-directed model and map validation for 3D cryo-electron microscopy. *Nat. Methods* **12**, 943–946 (2015).
126. D. Liebschner, P. V. Afonine, M. L. Baker, G. Bunkóczi, V. B. Chen, T. I. Croll, B. Hintze, L. W. Hung, S. Jain, A. J. McCoy, N. W. Moriarty, R. D. Oeffner, B. K. Poon, M. G. Prisant, R. J. Read, J. S. Richardson, D. C. Richardson, M. D. Sammito, O. V. Sobolev, D. H. Stockwell, T. C. Terwilliger, A. G. Urzhumtsev, L. L. Videau, C. J. Williams, P. D. Adams, Macromolecular structure determination using x-rays, neutrons and electrons: Recent developments in Phenix. *Acta Crystallogr. D Struct. Biol.* **75**, 861–877 (2019).
127. J. Agirre, J. Iglesias-Fernández, C. Rovira, G. J. Davies, K. S. Wilson, K. D. Cowtan, Privateer: Software for the conformational validation of carbohydrate structures. *Nat. Struct. Mol. Biol.* **22**, 833–834 (2015).
128. T. D. Goddard, C. C. Huang, E. C. Meng, E. F. Pettersen, G. S. Couch, J. H. Morris, T. E. Ferrin, UCSF ChimeraX: Meeting modern challenges in visualization and analysis. *Protein Sci.* **27**, 14–25 (2018).
- Pathogenesis of Infectious Disease Awards from the Burroughs Wellcome Fund (D.V.), Fast Grants (D.V.), the Bill & Melinda Gates Foundation (OPP1156262 to D.V.), the University of Washington Arnold and Mabel Beckman Cryo-EM Center, and the NIH grant S100D032290 (to D.V.) and grant U01 AI151698 for the UWARN as part of the Centers for Research in Emerging Infectious Diseases (CREID) Network. D.V. is an Investigator of the Howard Hughes Medical Institute. **Author contributions:** J.E.B., A.C.W., M.A.T., and D.V. conceived the project and designed experiments. J.E.B., C. Stewart, J.T.B., W.K.S., and A.J. carried out ELISAs. J.E.B. performed antibody depletion experiments. J.E.B. and K.R.S. produced pseudotyped viruses. J.E.B., C. Stewart, J.T.B., W.K.S., and A.J. expressed and purified proteins. Y.-J.P. carried out cryoEM specimen preparation and data collection and processing. Y.-J.P. and D.V. built and refined the atomic models. A.C.W., M.M., N.M.F., J.K.L., I.G.M., A.W.N., R.P.S., Y.H., J.S.L., J.J., S.W.T., K.A., A. Shariq, J.M.D., Z.Z., D.W., A. Sette, G.S., C.M.P., N.T.I., J.G., A.B., A.G., F.S., J.A.M., S.C., W.C.V.V., C. Simmerling, R.G., H.Y.C., and D.C. provided unique reagents. D.V. supervised the project and obtained funding. J.E.B. and D.V. analyzed the data and wrote the manuscript with input from all authors. **Competing interests:** G.S. and D.C. are employees of Vir Biotechnology Inc. and may hold shares in Vir Biotechnology Inc. A.C.W. and D.V. are named as inventors on patent applications filed by the University of Washington for SARS-CoV-2 and sarbecovirus RBD nanoparticle vaccines (WO2021163438 and 63/378,410). H.Y.C. reported consulting with Ellume, Pfizer, the Bill and Melinda Gates Foundation, Glaxo Smith Kline, and Merck. She has received research funding from Emergent Ventures, Gates Ventures, Sanofi Pasteur, and the Bill and Melinda Gates Foundation and support and reagents from Ellume and Cepheid outside of the submitted work. R.P.S., Y.H., A.W.N., and J.A.M. are named as inventors on a patent application for broadly reactive sarbecovirus S<sub>2</sub>-binding antibodies (63/135,913), and J.A.M. is an inventor on a patent for stabilized coronavirus spike proteins (63/032,502) filed by the University of Texas. The remaining authors declare that the research was conducted in the absence of any commercial or financial relationships that could be construed as a potential conflict of interest. **Data and materials availability:** The cryoEM map and coordinates have been deposited to the Electron Microscopy Data Bank and PDB with the accession numbers EMD-27779 and PDB 8DYA. Plasmids generated in this study will be made available on request but may require a completed materials transfer agreement signed with Vir Biotechnology or the University of Washington. All other data needed to support the conclusions in the paper are present in the paper or the Supplementary Materials. This work is licensed under a Creative Commons Attribution 4.0 International (CC BY 4.0) license, which permits unrestricted use, distribution, and reproduction in any medium, provided the original work is properly cited. To view a copy of this license, visit <http://creativecommons.org/licenses/by/4.0/>. This license does not apply to figures/photos/artwork or other content included in the article that is credited to a third party; obtain authorization from the rights holder before using such material.

**Acknowledgments:** We thank H. Tani (University of Toyama) for providing the reagents necessary for preparing VSV pseudotyped viruses. **Funding:** This study was supported by the National Institute of Allergy and Infectious Diseases (DP1AI158186 and 75N93022C00036 to D.V. and U01 AI151698 to W.C.V.V.), the National Institute of General Medical Sciences (R01GM120553 to D.V.), a Pew Biomedical Scholars Award (D.V.), an Investigator in the

Submitted 1 October 2022  
Accepted 7 November 2022  
Published 23 December 2022  
10.1126/sciimmunol.adf1421

## **SARS-CoV-2 spike conformation determines plasma neutralizing activity elicited by a wide panel of human vaccines**

John E. Bowen, Young-Jun Park, Cameron Stewart, Jack T. Brown, William K. Sharkey, Alexandra C. Walls, Anshu Joshi, Kaitlin R. Sprouse, Matthew McCallum, M. Alejandra Tortorici, Nicholas M. Franko, Jennifer K. Logue, Ignacio G. Mazzitelli, Annalee W. Nguyen, Rui P. Silva, Yimin Huang, Jun Siong Low, Josipa Jerak, Sasha W. Tiles, Kumail Ahmed, Asefa Shariq, Jennifer M. Dan, Zeli Zhang, Daniela Weiskopf, Alessandro Sette, Gyorgy Snell, Christine M. Posavad, Najeeha Talat Iqbal, Jorge Geffner, Alessandra Bandera, Andrea Gori, Federica Sallusto, Jennifer A. Maynard, Shane Crotty, Wesley C. Van Voorhis, Carlos Simmerling, Renata Grifantini, Helen Y. Chu, Davide Corti, and David Veesler

*Sci. Immunol.*, **7** (78), eadf1421.

DOI: 10.1126/sciimmunol.adf1421

### **View the article online**

<https://www.science.org/doi/10.1126/sciimmunol.adf1421>

### **Permissions**

<https://www.science.org/help/reprints-and-permissions>

Use of this article is subject to the [Terms of service](#)

---

*Science Immunology* (ISSN ) is published by the American Association for the Advancement of Science. 1200 New York Avenue NW, Washington, DC 20005. The title *Science Immunology* is a registered trademark of AAAS.

Copyright © 2022 The Authors, some rights reserved; exclusive licensee American Association for the Advancement of Science. No claim to original U.S. Government Works. Distributed under a Creative Commons Attribution License 4.0 (CC BY).